Singapore Management University

Institutional Knowledge at Singapore Management University

Research Collection School Of Economics | School of Economics

1-2024

On the optimal forecast with the fractional Brownian motion

Xiaohu WANG

Jun YU
Singapore Management University, yujun@smu.edu.sg

Chen ZHANG
Singapore Management University, chenzhang@smu.edu.sg

Follow this and additional works at: https://ink.library.smu.edu.sg/soe_research

 Part of the Econometrics Commons

Citation

WANG, Xiaohu; Jun YU; and ZHANG, Chen. On the optimal forecast with the fractional Brownian motion. (2024). *Quantitative Finance*. 24, (2), 337-346.
Available at: https://ink.library.smu.edu.sg/soe_research/2751

This Journal Article is brought to you for free and open access by the School of Economics at Institutional Knowledge at Singapore Management University. It has been accepted for inclusion in Research Collection School Of Economics by an authorized administrator of Institutional Knowledge at Singapore Management University. For more information, please email cherylds@smu.edu.sg.

On the Optimal Forecast with the Fractional Brownian Motion*

Xiaohu Wang
Fudan University
Jun Yu, Chen Zhang
Singapore Management University

May 9, 2023

Abstract

This paper investigates the performance of different forecasting formulas with fractional Brownian motion based on discrete and finite samples. Existing literature presents two formulas for generating optimal forecasts when continuous records are available. One formula relies on a history over an infinite past, while the other is designed for a record limited to a finite past. However, when discrete-time observations over a finite past are available, various discretization schemes are proposed to approximate the forecasting formulas that rely on continuous records. This study compares the forecasts generated by these alternative discretization schemes with the forecasts derived from the conditional expectation of the target variable using a discrete and finite sample. The findings indicate that the conditional expectation approach produces more accurate forecasts compared to the discretization-based

*We wish to thank Mathieu Rosenbaum, Shuping Shi, Weilin Xiao and Masaaki Fukasawa for helpful comments. Xiaohu Wang, School of Economics, Fudan University, Shanghai, China, and Shanghai Institute of International Finance and Economics, Shanghai, China, Email: wang_xh@fudan.edu.cn. Jun Yu, School of Economics and Lee Kong Chian School of Business, Singapore Management University, 90 Stamford Road, Singapore 178903. Email: yujun@smu.edu.sg. Chen Zhang, School of Economics, Singapore Management University, 90 Stamford Road, Singapore 178903. Email: chenzhang@smu.edu.sg. Wang acknowledges the support by Shanghai Pujiang Program under No.22PJC022. Yu and Zhang would like to acknowledge that this research/project is supported by the Ministry of Education, Singapore, under its Academic Research Fund (AcRF) Tier 2 (Award Number MOE-T2EP402A20-0002).

formulas, as demonstrated by both simulated data and actual daily realized volatility (RV) observations. Since the discretization-based formula is widely applied in the rough volatility literature, our empirical results, which favor the conditional expectation approach, reinforce the already well-established effectiveness of fractional Brownian motion in forecasting future RV.

JEL classification: C12, C22, G01
Keywords: Fractional Gaussian noise; Conditional expectation; Anti-persistence; Continuous record; Discrete record; Optimal forecast

1 Introduction

The volatility literature, particularly since the groundbreaking paper by Gatheral et al. (2018), has consistently demonstrated the superior forecasting accuracy of continuous-time models based on rough fractional Brownian motion (fBm) when compared to popular discrete-time models. Notably, Gatheral et al. (2018) show that the rough fBm model, with a Hurst parameter (denoted as H) equal to 0.14, outperforms the HAR model by Corsi (2009) in forecasting realized volatility (RV) and log realized volatility (RV). Wang et al. (2023) contribute additional empirical evidence supporting the effectiveness of rough fBm and rough fractional Ornstein-Uhlenbeck (fOU) processes in forecasting log RV and RV, surpassing the HAR and ARFIMA models. In their study, Wang et al. (2023) estimate the Hurst parameter H recursively using the method-of-moments approach based on daily log RV data. Their results consistently indicate that H is significantly less than 0.5. Similarly, based on a maximum composite likelihood method and the Whittle maximum likelihood method, respectively, Bennedsen et al. (2022) and Shi et al. (2023) propose to estimate the fOU process and corroborate the finding of $H < 0.5$. Furthermore, Fukasawa et al. (2022) and Bolko et al. (2023) independently confirm the evidence of $H < 0.5$, even when considering measurement errors in RV.

The fBm with $H < 0.5$, known for generating sample paths rougher than standard Brownian motion, is commonly referred to as the rough fractional stochastic volatility (RFSV) model when applied to model volatility. The RFSV literature has garnered significant attention across mathematical finance, financial engineering, and financial econometrics. In recognition of their pioneering work, Jim Gatheral and Mathieu Rosenbaum were awarded the 2021 risk award for introducing this

model, highlighting its importance and impact in the field. A dedicated website has been established to compile the extensive literature on RFSV, featuring over 200 papers that explore this subject from various perspectives.[1] In addition to its applications in volatility forecasting, RFSV models have been utilized in options pricing (Livieri et al., 2018; Bayer et al., 2016; Garnier and Sølna, 2017) and variance swaps (Bayer et al., 2016), portfolio choice (Fouque and Hu, 2018), and dynamic hedging (Euch and Rosenbaum, 2018).

This paper focuses on evaluating the performance of alternative forecasting formulas with fBm based on discrete and finite samples. In situations where continuous records of fBm are accessible, the literature has derived two formulas that generate optimal forecasts. One formula is applicable when an infinite history is observed, while the other is designed for continuous records over a finite period. Both formulas involve the integration of the continuous record with specific weighting functions. However, in practice, only limited discrete-time observations over a finite past are available, posing a challenge for implementing these formulas directly. To address this limitation, Gatheral et al. (2018) introduced a specific Riemann sum approximation approach to forecast volatility in real-world settings. This approximation method, derived from the forecasting formula for the continuous record over the infinite past, has gained significant prominence and is now widely adopted in the volatility forecasting literature.

In this paper, we investigate the performance of various discrete-time approximation schemes applied to the two forecasting formulas mentioned earlier. We compare the forecasts generated by these approximation schemes with the forecasts obtained by directly using the conditional expectation of the target variable on the vector of discrete-time data. Our analysis includes both simulated data experiments and empirical studies. Our results indicate that the existing forecasting formulas, which are optimal when continuous records are available, exhibit inferior performance when applied to generate forecasts based on limited discrete-time data. Conversely, we find that utilizing the conditional expectation directly on the vector of discrete-time data yields optimal forecasts. These findings highlight the importance of incorporating discrete-time data directly into the forecasting process, rather than relying on the discretization of continuous records. Furthermore, our paper suggests that the rough fBm model has the potential to produce even more accurate forecasts of

[1] https://sites.google.com/site/roughvol/home/risks-1

log RV than what has been previously reported in the literature. Consequently, our findings contribute to enhancing the already well-established reputation of fBm for its remarkable performance in forecasting volatility.

The rest of the paper is organized as follows. Section 2 reviews the model and discusses the alternative forecasting formulas. Section 3 compares the forecasting performance of alternative methods based on simulated data. Section 4 reports the forecasting results of alternative methods based on real RV data. Section 5 concludes. The appendix contains a proof of the Proposition in the the main body of the paper.

2 The Model and Forecasting Formulas

The process considered in the paper is a scaled fBm, denoted by $\sigma B^H(t)$, which is a continuous-time Gaussian process with zero mean and the autocovariance function of

$$Cov\left(B^H(t), B^H(s)\right) = \frac{1}{2}\left(|t|^{2H} + |s|^{2H} - |t-s|^{2H}\right), \quad \forall t, s \in (-\infty, +\infty), \qquad (1)$$

where $\sigma > 0$ is a constant scale parameter and $H \in (0,1)$ is the Hurst parameter of the fBm. An alternative definition of $B^H(t)$, given by Mandelbrot and Van Ness (1968), is

$$B^H(t) = \frac{1}{\Gamma(H+0.5)}\left\{\int_{-\infty}^{0}\left[(t-s)^{H-0.5} - (-s)^{H-0.5}\right]dW(s) + \int_0^t (t-s)^{H-0.5}\,dW(s)\right\},$$

where $\Gamma(\cdot)$ denotes the Gamma function and $W(t)$ is a standard Brownian motion. In the special case of $H = 1/2$, the fBm becomes a standard Brownian motion, that is $B^{1/2}(r) = W(r)$.

Define the increments of the fBm as $y_t \equiv \sigma\left(B^H(t) - B^H(t-1)\right)$ with t taking values of positive integers. The sequence $\{y_t\}$ is known in the literature as the fractional Gaussian noise (fGn), which is a normally distributed stationary process with the following autocovariance function:

$$\begin{aligned} Cov\left(y_t, y_{t+k}\right) &= \frac{\sigma^2}{2}\left((k+1)^{2H} + (k-1)^{2H} - 2k^{2H}\right), \text{ for any } k \geq 0 \qquad (2)\\ &\sim \sigma^2 H(2H-1)k^{2H-2} \text{ for large } k. \end{aligned}$$

where $\sim$ denotes asymptotic equivalence. From Equation (2), it can be seen that when $H \in (0.5, 1)$, $\{y_t\}$ has positive serial dependence, and the autocovariances of $\{y_t\}$ are not summable. As a result, $\{y_t\}$ is a long-memory process when $H > 0.5$. In contrast, when $H \in (0, 0.5)$, $Cov\left(y_t, y_{t+k}\right) < 0$ for all $k \neq 0$ and $\sum_{k=-\infty}^{+\infty} Cov\left(y_t, y_{t+k}\right) = 0$. In this case, $\{y_t\}$ is called an antipersistent process.

Gehringer and Li (2020) prove that the sample path of $\sigma B^H(t)$ is (locally) Hölder continuous of order $H - \epsilon$with ϵ being a positive number arbitrarily close to zero. That means when $H < 0.5$, the sample path of $\sigma B^H(t)$ is rougher than that of a standard Brownian motion. For this reason, any model involving an fBm with $H < 0.5$ to fit the volatility of financial assets is called a rough volatility model. Empirical studies in the volatility literature have found ample evidence supporting roughness (i.e., $H < 0.5$); see, e.g., Bayer et al. (2016) and Gatheral et al. (2018). Our paper, therefore, focuses on generating optimal forecasts of $\sigma B^H(t)$ when $H < 0.5$.

Various methods have been developed to generate out-of-sample forecasts of $\sigma B^H(t)$. The most commonly employed method in the literature is based on the formula introduced by Gatheral et al. (2018). However, it is important to note that this formula does not necessarily provide the optimal forecast. The following subsections will introduce alternative forecasting methods, explore their differences, and point out the one that generates optimal forecasts that minimize the root mean squared error (RMSE).

2.1 Forecasts based on the infinite-past-formula

When a continuous-time record of $X(t) \equiv \sigma B^H(t)$over the period of $(-\infty, T]$ is available, Nuzman and Poor (2000, Equation (34)) develop the formula of the conditional expectation of $X(T+k)$ to generate the optimal k-period-ahead forecast:

$$E\left\{X\left(T+k\right)|X(t), t \in (-\infty, T]\right\} = \int_{-\infty}^{T} \frac{\cos(H\pi)k^{H+0.5}}{\pi(T-s+k)(T-s)^{H+0.5}} X(s)ds. \quad (3)$$

where k is any positive number. The forecasting formula is a weighted average of the entire history of $X(t)$ over $(-\infty, T]$. The following proposition shows that for any $T > 0$ and $k > 0$, the weights in the forecasting formula integrated to unity.

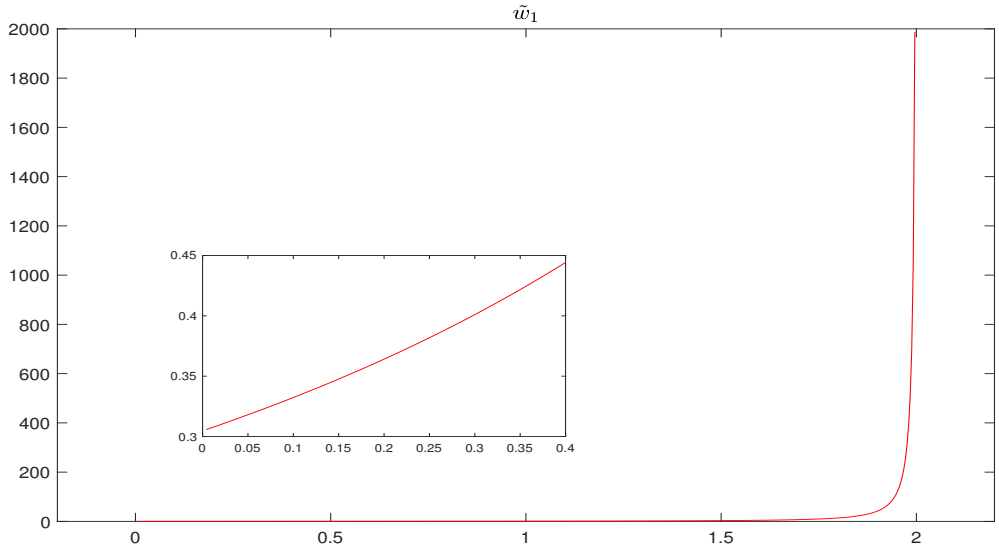

Figure 1: Plot of $\widetilde{w}_1(s)$ as a function of s when $H = 0.2$, $k = 1/50$, $T = 2$. The picture-in-picture plots $\widetilde{w}_1(s)$ when s takes values close to zero.

Proposition 2.1 *For any $T, k > 0$, it has*

$$\int_{-\infty}^{T} \frac{\cos(H\pi)k^{H+0.5}}{\pi(T-s+k)(T-s)^{H+0.5}} ds = 1.$$

To simplify the notation, define

$$w_1(s) \equiv \frac{\cos(H\pi)k^{H+0.5}}{\pi(T-s+k)(T-s)^{H+0.5}} = \frac{\cos(H\pi)k^{H+0.5}}{\pi} \widetilde{w}_1(s),$$

with

$$\widetilde{w}_1(s) \equiv \frac{1}{(T-s+k)(T-s)^{H+0.5}}.$$

The forecasting formula in (3) can be rewritten as

$$\begin{aligned} E\left\{X\left(T+k\right)|X(t), t \in (-\infty, T]\right\} &= \int_{-\infty}^{T} w_1(s)X(s)ds \\ &= \frac{\cos(H\pi)k^{H+0.5}}{\pi} \int_{-\infty}^{T} \widetilde{w}_1(s)X(s)ds. \quad (4) \end{aligned}$$

Figure 1 plots $\widetilde{w}_1(s)$ as a function of $s \in [0, T]$ when $H = 0.2$, $k = 1/50$, and $T = 2$. To help understand the near-zero behavior of $\widetilde{w}_1(s)$, we plot $\widetilde{w}_1(s)$

when s takes values close to zero in a subfigure. The figure shows that $\widetilde{w}_1(s)$ is a monotonically increasing function that goes to ∞ as $s \to T$. This property suggests that nearer-distant history is more important than further-distant history in forecasting $X(T+k)$.

In practice, however, it is infeasible to directly implement Formula (4) to generate forecasts. First of all, it is impossible to possess the information in the infinite past. Second, we live in a digital world. Instead of having a continuous record of $X(t)$, interested variables in financial markets can only be observed at discrete time points. Therefore, in reality, people can only generate forecasts based on a discrete record of $X(t)$ collected over the finite time-interval $[0, T]$. Without loss of generality, we use $\{X_0, X_1, ..., X_T\}$ to denote the data available.

Gatheral et al. (2018) propose a forecasting formula based on the discrete record $\{X_0, X_1, ..., X_T\}$ by making three adjustments to the formula in (4). The first adjustment is to truncate the integral from below at zero, which gives the first approximation in (5). The second adjustment is to approximate the integral with a particular type of Riemann sum. In each time interval $[s-1, s]$, the weight takes the value at the left point, and the observation takes the value at the right point, which leads to the second approximation in (5).

$$\begin{aligned} & E\left\{X\left(T+k\right)|X(t), t \in (-\infty, T]\right\} = \int_{-\infty}^{T} w_1(s)X(s)ds \\ \approx & \int_{0}^{T} w_1(s)X(s)ds = \sum_{s=1}^{T}\int_{s-1}^{s} w_1(\tau)X(\tau)d\tau \approx \sum_{s=1}^{T} w_1(s-1)X_s. \end{aligned} \tag{5}$$

To mimic the feature in Proposition 2.1, which helps to reduce the truncation error introduced by the first adjustment, Gatheral et al. (2018) suggest normalizing the sum of the weights in (4) to be one. The final forecasting formula given by Gatheral et al. (2018) is[2]

$$IPGA = \frac{\sum_{s=1}^{T} w_1(s-1)X_s}{\sum_{s=1}^{T} w_1(s-1)} = \frac{\sum_{s=1}^{T} \widetilde{w}_1(s-1)X_s}{\sum_{s=1}^{T} \widetilde{w}_1(s-1)}. \tag{6}$$

In the present paper, we name it the infinite-past-Gatheral-adjustment (IPGA) forecasting formula. This formula is the one commonly applied in the rough volatility

[2]We are grateful to Mathieu Rosenbaum to confirm that this formula is the same as the one used in Gatheral et al. (2018).

literature.

Note that many alternative types of Riemann sum may be used to approximate the integral in (4). The IPGA formula can be generalized by allowing the weight $w_1(\tau)$ to take any value in the interval of $[s-1, s]$. The generalized forecasting formula, named as infinite-past-ϵ-adjustment (IPϵA) formula, takes the form of

$$IP\epsilon A = \frac{\sum_{s=1}^{T} w_1(s-1+\epsilon)X_s}{\sum_{s=1}^{T} w_1(s-1+\epsilon)} = \frac{\sum_{s=1}^{T} \widetilde{w}_1(s-1+\epsilon)X_s}{\sum_{s=1}^{T} \widetilde{w}_1(s-1+\epsilon)}, \tag{7}$$

where ϵ can be any number in $[0, 1]$. Clearly, when $\epsilon = 0$, the $IP\epsilon A$ formula is the same as the IPGA formula.

Letting $\epsilon = 1$, it leads to an alternative forecasting formula as

$$IP\epsilon A_{\epsilon=1} \equiv IPRA = \frac{\sum_{s=1}^{T-1} \widetilde{w}_1(s)X_s + \widetilde{w}_1(T-1)X_T}{\sum_{s=1}^{T-1} \widetilde{w}_1(s) + \widetilde{w}_1(T-1)}. \tag{8}$$

Note that the weight function $\widetilde{w}_1(s)$ is not well-defined at the point $s = T$. Therefore, in the last term of the Riemann summation, we use $\widetilde{w}_1(T-1)$, instead of $\widetilde{w}_1(T)$, as the weight. Except for the last time interval, the $IP\epsilon A$ with $\epsilon = 1$ uses the value of $\widetilde{w}_1(\tau)X(\tau)$ at the right point to approximate $\int_{s-1}^{s} \widetilde{w}_1(\tau)X(\tau)d\tau$. Hence, this forecasting formula is named the infinite-past-right-adjustment (IPRA) formula.

To better understand the importance of the weight choice in generating forecasts through simulation and empirical studies, we also give the explicit expression of the $IP\epsilon A$ formula with $\epsilon = 1/2$:

$$IP\epsilon A_{\epsilon=\frac{1}{2}} \equiv IPMA = \frac{\sum_{s=1}^{T} \widetilde{w}_1(s-1+\frac{1}{2})X_s}{\sum_{s=1}^{T} \widetilde{w}_1(s-1+\frac{1}{2})}. \tag{9}$$

We name this formula the infinite-past-middle-adjustment (IPMA).

Another widely used method to approximate the integral of $\int_{s-1}^{s} \widetilde{w}_1(\tau)X(\tau)d\tau$ is to use the trapezoidal sum, i.e., $\left(w_1(s-1)X_{s-1} + w_1(s)X_s\right)/2$. We hence get another alternative forecasting formula:

$$IPTA = \frac{\frac{1}{2}\widetilde{w}_1(0)X_0 + \sum_{s=1}^{T-1} \widetilde{w}_1(s)X_s + \frac{1}{2}\widetilde{w}_1(T-1)X_T}{\frac{1}{2}\widetilde{w}_1(0) + \sum_{s=1}^{T-2} \widetilde{w}_1(s) + \frac{3}{2}\widetilde{w}_1(T-1)}. \tag{10}$$

This is named the infinite-past-trapezoidal-adjustment (IPTA) method.

It is important to remark that, although Formula (4) yields the optimal forecast given a continuous record over $(-\infty, T]$ being available, the alternative discretizations given in (6)-(10) may not lead to the optimal forecast when only a finite number of discrete-time observations $\{X_0, X_{1,}..., X_T\}$ are available. In fact, they are not designed to minimize any objective function of the forecast errors.

2.2 Forecasts based on the finite-past-formula

If the process $X(t) = \sigma B^H(t)$ has a continuous record available over only the finite period of $[0, T]$, Theorem 4.4 in Nuzman and Poor (2000) derives the conditional-mean formula of $X(T+k)$ for any $k > 0$ to generate the k-period-ahead optimal forecast at period T:

$$\begin{aligned} E\left\{X\left(T+k\right)|X(t), t \in [0,T]\right\} &= \int_0^T m_T\left(\frac{k}{T}, T-s\right) X(s)ds, \\ &= \int_0^T w_2(s)X(s)ds, \end{aligned} \tag{11}$$

where

$$w_2(s) \equiv m_T\left(\frac{k}{T}, T-s\right),$$

and

$$\begin{aligned} m_T(c,t) = T^{-1}&\left(\frac{t}{T}\right)^{-H-0.5}\left(1-\frac{t}{T}\right)^{-H-0.5} \\ &\times\left[(0.5-H)B_{c/(c+1)}\left(H+0.5, 1-2H\right) + \frac{c^{H+0.5}(1+c)^{H-0.5}(1-t/T)}{c+t/T}\right], \end{aligned}$$

with $B_{c/(c+1)}(\cdot,\cdot)$ denoting the incomplete beta function that takes the form of

$$B_{c/(c+1)}\left(H+0.5, 1-2H\right) = \int_0^{c/(c+1)} z^{H-0.5}\left(1-z\right)^{-2H} dz.$$

The forecasting formula in (11) is a weighted average of the available history of $X(t)$ over $[0, T]$. It is verified, as noted on page 443 in Nuzman and Poor (2000), that the integral of the weights over the interval [0, T] equals one as

$$\int_0^T m_T(c,t)dt = 1 \quad \text{for any} \quad T, c > 0.$$

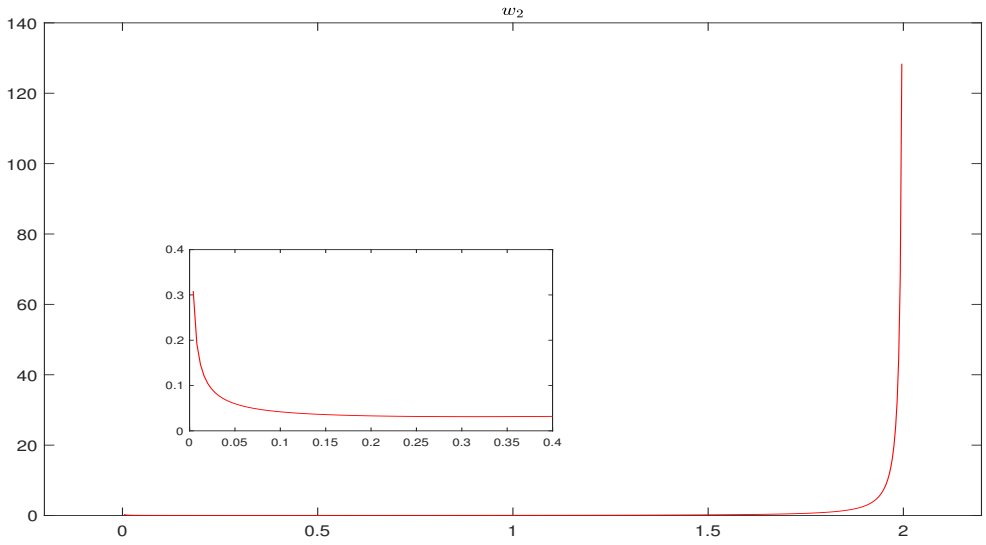

Figure 2: Plots of $w_2(s)$ as a function of s when $H = 0.2, k = 1/50, T = 2$. The picture-in-picture plots $w_2(s)$ when s takes values close to zero.

From the definition of $w_2(s)$, it is easy to get that $\lim_{s\to 0} w_2(s) = \infty$ and $\lim_{s\to T} w_2(s) = \infty$ when $H \in (0, 0.5)$. As a result, $w_2(s)$ is not a monotonic function. It is a little surprising to see that $w_2(s)$ approaches infinity as $s \to 0$. This feature is sharply distinct from the weights function $\widetilde{w}_1(s)$ used in the forecast formula (4) that converges to a small constant number when $s \to 0$, as discussed in Subsection 2.1. This difference is due to the fact that the new forecasting formula in (11) is based on a continuous record over $[0, T]$ rather than $(-\infty, T]$. When the record over $[0, T]$ being available, the forecasting formula (11) places the optimal weight $X(s)$ for $s \in (0, T)$. Hence, it can generate more accurate forecasts than using the forecasting formula (4) with a truncation from below at zero.

Figure 2 plots $w_2(s)$ as a function of s when $H = 0.2, k = 1/50$, and $T = 2$. It shows that when T is finite, $w_2(s)$ is U-shaped, placing higher weights when s approaches T or 0.

We plot the normalized $w_2(s)$ and $\widetilde{w}_1(s)$, i.e. $w_2(s)/\int_0^T w_2(\tau)d\tau$ and $\widetilde{w}_1(s)/\int_0^T \widetilde{w}_1(\tau)d\tau$, as a function of s in Figure 3, for $k = 1/250, 1/50$ and $T = 2, 4$, respectively. Doing normalization ensures the weights calculated at discrete points sum to unity.[3] These

[3]Although $\int_0^T w_2(\tau)d\tau = 1$, normalizing $w_2(\tau)$ is necessary as the numerical approximation to $\int_0^T w_2(\tau)d\tau$ can be different from one.

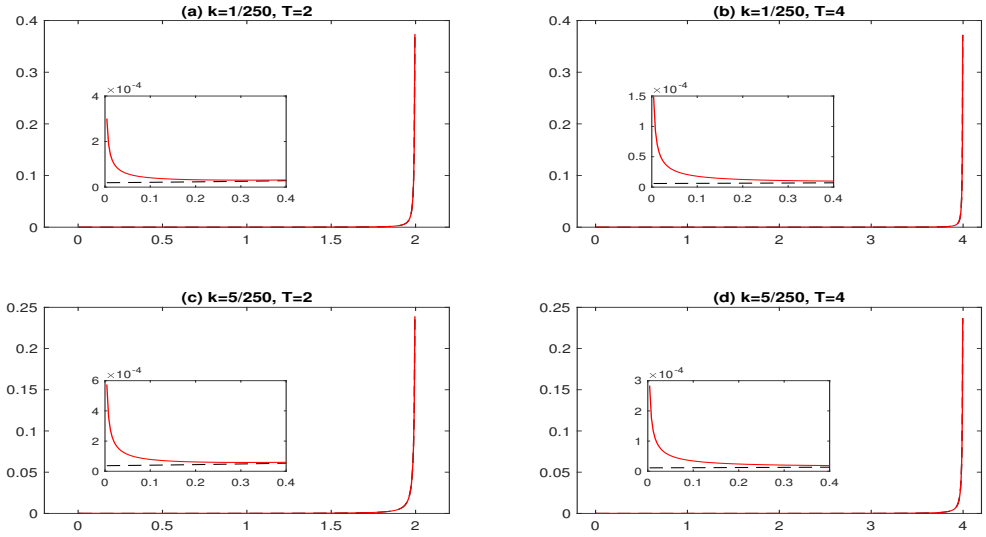

Figure 3: Plots of normalized $\widetilde{w}_1(s)$ and $w_2(s)$ as a function of s when $H = 0.2$, $k = 1/250, 1/50$ and $T = 2, 4$. The solid line is for normalized $w_2(s)$ while the dash line is for normalized $\widetilde{w}_1(s)$. The picture-in-picture plots each weight function when s takes values close to zero.

plots show that compared to $\widetilde{w}_1(s)/\int_0^T \widetilde{w}_1(\tau)d\tau$, the normalized weight function of $w_2(s)/\int_0^T w_2(\tau)d\tau$ places higher weights on observations near the initial period.

When only discrete-time observations $\{X_0, ..., X_T\}$ are available, the forecasting formula in (11) can not be applied directly. Riemann sums may be used to approximate the integral in the formula of (11). In each subinterval $[s-1, s]$, where $s = 1, 2, \ldots, T$, we choose the observation at the right time point X_s, the weight at the point of $s - 1 + \epsilon$ with $\epsilon \in [0, 1]$, and use their product to approximate the integral. After normalizing the weights to have a unity summation, the so-called finite-past-ϵ-adjustment (FPϵA) forecasting formula is obtained as

$$FP\epsilon A = \frac{\sum_{s=1}^{T} w_2(s-1+\epsilon)X_s}{\sum_{s=1}^{T} w_2(s-1+\epsilon)}. \tag{12}$$

To better understand the impact of the weights chosen on forecasting performance, we consider three special choices for ϵ, i.e., $\epsilon = 0, 1/2, 1$. The resulting formulas are named finite-past-Gatheral-adjustment (FPGA),[4] finite-past-Middle-

[4]Note that $w_2(0) = \infty$. Hence, instead of taking $w_2(0)$ as the weight, we use $w_2(1)X_1$ to approximate the integral $\int_0^1 w_2(s)X(s)\,ds$.

adjustment (FPMA), and finite-past-right-adjustment(FPRA)[5] formula accordingly:

$$FP\epsilon A_{\epsilon=0} \equiv FPGA = \frac{\sum_{s=2}^{T} w_2(s-1)X_s + w_2(1)X_1}{\sum_{s=1}^{T} w_2(s-1) + w_2(1)}, \tag{13}$$

$$FP\epsilon A_{\epsilon=\frac{1}{2}} \equiv FPMA = \frac{\sum_{s=1}^{T} w_2\left(s-\frac{1}{2}\right)X_s}{\sum_{s=1}^{T} w_2\left(s-\frac{1}{2}\right)}, \tag{14}$$

and

$$FP\epsilon A_{\epsilon=1} \equiv FPRA = \frac{\sum_{s=1}^{T-1} w_2(s)X_s + w_2(T-1)X_T}{\sum_{s=1}^{T-1} w_2(s) + w_2(T-1)}. \tag{15}$$

In each subinterval $[s-1, s]$, the FPGA formula chooses the observation at the right point X_s and the weight at the left point $w_2(s-1)$, the FPMA adopts the weight at the middle point $w_2(s-1/2)$, and the FPRA applies the weight at the right point $w_2(s)$.

Another alternative method to approximate an integral is to use the trapezoidal sum, which leads to the following forecasting formula:

$$FPTA = \frac{\frac{1}{2}w_2(1)(X_0+X_1) + \frac{1}{2}\sum_{s=1}^{T-2}\left(w_2(s)X_s + w_2(s+1)X_{s+1}\right) + \frac{1}{2}w_2(T-1)(X_{T-1}+X_T)}{\sum_{s=2}^{T-2} w_2(s) + \frac{3}{2}\left(w_2(1)+w_2(T-1)\right)}. \tag{16}$$

We name this formula the finite-past-trapezoidal-adjustment (FPTA) formula.

Although Formula (11) yields the optimal forecast given a continuous record over $[0, T]$ being available, the alternative discretizations given in (13)-(14) may not lead to the optimal forecast when only finite number discrete-time observations $\{X_0, X_1, ..., X_T\}$ are available. None of these discretization-based formulas is designed to minimize any objective function of the forecast errors.

Table 1 reports the weights applied to all observations in the discrete sample under alternative forecasting formulas. It is worth noting that the derivative of $\tilde{w}_1(s)$ with respect to s is always positive, and the weights of IPϵA are always monotonically increasing regardless of the value of ϵ.

2.3 Optimal forecast based on a discrete and finite sample

This subsection introduces the optimal forecasting formula based on finite discrete-time observations $\{X_0, X_\Delta ..., X_{T\Delta}\}$, where Δ is the sampling interval and $T+1$ is the number of historical observations. Δ here represents the sampling frequency of

[5]Note that $w_2(T) = \infty$. Therefore, we approximate the integral $\int_{T-1}^{T} w_2(s)X(s)\,ds$ by using $X(T)$ with the weight of $w_2(T-1)$.

Table 1: Weights on the sample under different forecasting formulas before the normalization

Methods	X_0	X_1	X_2	$\cdots$	X_{T-2}	X_{T-1}	X_T
IPGA	0	$\widetilde{w}_1(0)$	$\widetilde{w}_1(1)$	$\cdots$	$\widetilde{w}_1(T-3)$	$\widetilde{w}_1(T-2)$	$\widetilde{w}_1(T-1)$
IPRA	0	$\widetilde{w}_1(1)$	$\widetilde{w}_1(2)$	$\cdots$	$\widetilde{w}_1(T-2)$	$\widetilde{w}_1(T-1)$	$\widetilde{w}_1(T-1)$
IPTA	$\frac{1}{2}\widetilde{w}_1(0)$	$\widetilde{w}_1(1)$	$\widetilde{w}_1(2)$	$\cdots$	$\widetilde{w}_1(T-2)$	$\widetilde{w}_1(T-1)$	$\frac{1}{2}\widetilde{w}_1(T-1)$
IPMA	0	$\widetilde{w}_1(0.5)$	$\widetilde{w}_1(1.5)$	$\cdots$	$\widetilde{w}_1(T-2.5)$	$\widetilde{w}_1(T-1.5)$	$\widetilde{w}_1(T-0.5)$
FPGA	0	$w_2(0)$	$w_2(1)$	$\cdots$	$w_2(T-3)$	$w_2(T-2)$	$w_2(T-1)$
FPRA	0	$w_2(1)$	$w_2(2)$	$\cdots$	$w_2(T-2)$	$w_2(T-1)$	$w_2(T-1)$
FPTA	$\frac{1}{2}w_2(1)$	$w_2(1)$	$w_2(2)$	$\cdots$	$w_2(T-2)$	$w_2(T-1)$	$\frac{1}{2}w_2(T-1)$
FPMA	0	$w_2(0.5)$	$w_2(1.5)$	$\cdots$	$w_2(T-2.5)$	$w_2(T-1.5)$	$w_2(T-0.5)$

the observations. In the volatility literature, the length of a year is conventionally normalized to 1. Hence, when $\Delta = 1, 1/12, 1/252$, $X_{t\Delta}$ for $t = 0, 1, \ldots, T+1$ represents yearly, monthly, and daily observations accordingly. We summarize the data into a column vector $X = (X_0, X_\Delta ..., X_{T\Delta})'$. Our goal is to generate the optimal forecast for $X_{(T+k)\Delta}$, that is, k-period-ahead forecast that minimizes the RMSE.[6]

[6]By letting $\Delta = 1$, Subsections 2.1-2.2 introduce the forecasting formulas (6)-(9) and (13)-(14) that are obtained by discretizing the continuous-time integrals given in (4) and (11) respectively. It is important to note that those forecasting formulas apply when $\Delta \neq 1$. Take the formulas of (6) as an example. If $\Delta \neq 1$, the expectation of $X[(T+k)\Delta]$ conditional on the observations over $(-\infty, T\Delta]$ derived by Nuzman and Poor (2000) becomes

$$\begin{aligned} & E\{X[(T+k)\Delta] \,|X(t), t \in (-\infty, T\Delta]\} \\ = & \int_{-\infty}^{T\Delta} \frac{\cos(H\pi)(k\Delta)^{H+0.5}}{\pi(T\Delta - s + k\Delta)(T\Delta - s)^{H+0.5}} X(s)ds = \int_{-\infty}^{T\Delta} w_1(s)X(s)ds \\ \approx & \int_0^{T\Delta} w_1(s)X(s)ds = \sum_{s=1}^{T} \int_{(s-1)\Delta}^{s\Delta} w_1(\tau)X(\tau)d\tau \approx \sum_{s=1}^{T} w_1[(s-1)\Delta] X_{s\Delta} \end{aligned}$$

Hence, the forecasting formula should be

$$\frac{\sum_{s=1}^{T} w_1[(s-1)\Delta] X_{s\Delta}}{\sum_{s=1}^{T} w_1[(s-1)\Delta]} = \frac{\sum_{s=1}^{T} w_1(s-1)X_{s\Delta}}{\sum_{s=1}^{T} w_1(s-1)} = IPGA$$

where the first equation comes from the fact that

$$w_1[(s-1)\Delta] = \frac{\cos(H\pi)(k\Delta)^{H+0.5}}{\pi(T\Delta - (s-1)\Delta + k\Delta)(T\Delta - (s-1)\Delta)^{H+0.5}} = \frac{1}{\Delta} w_1(s-1),$$

and

$$\frac{w_1[(s-1)\Delta]}{\sum_{s=1}^{T} w_1[(s-1)\Delta]} = \frac{w_1(s-1)}{\sum_{s=1}^{T} w_1(s-1)}.$$

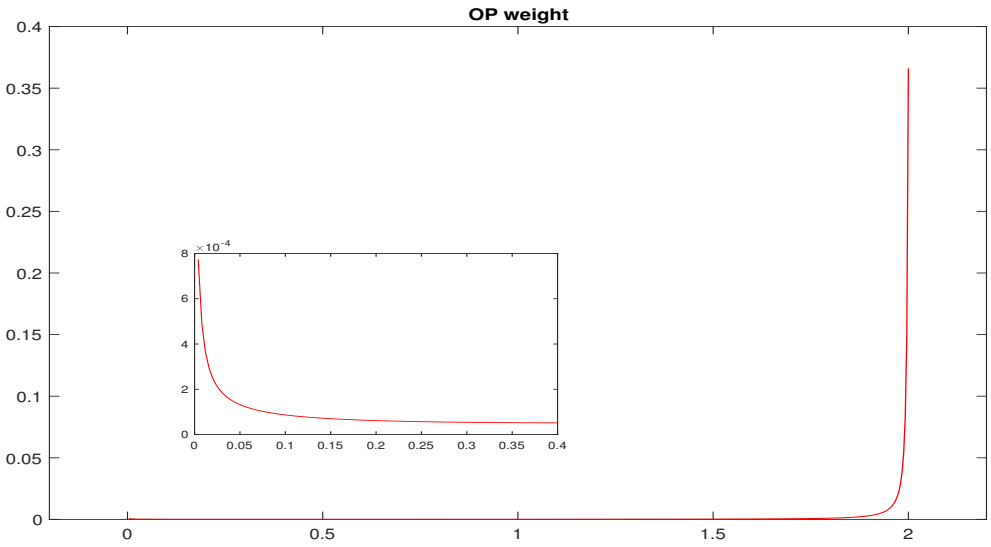

Figure 4: Optimal weight as a function of $s \in \{0, \Delta, 2\Delta, ..., T\Delta\}$ when $H = 0.2$, $k\Delta = 1/50$, $T\Delta = 2$.

Let $\Sigma_{0:T\Delta}$ denote the covariance matrix of X. Elements in $\Sigma_{0:T\Delta}$ can be easily obtained from the formula in (1). Define $\gamma_{k\Delta}^{(0:T\Delta)} = (Cov(X_{(T+k)\Delta}, X_0), ..., Cov(X_{(T+k)\Delta}, X_{T\Delta}))'$ as the vector of covariances between $X_{(T+k)\Delta}$ and the elements in X. Again, elements in $\gamma_{k\Delta}^{(0:T\Delta)}$ can readily be obtained from (1). Since X_t is a Gaussian process, the vector of $(X_0, X_\Delta, ..., X_{T\Delta}, X_{(T+k)\Delta})'$ follows a multivariate normal distribution. The expectation of $X_{(T+k)\Delta}$ conditional on X has a closed-form expression, which takes the form of

$$E(X_{(T+k)\Delta}|X) = \left(\gamma_{k\Delta}^{(0:T\Delta)}\right)' \Sigma_{0:T\Delta}^{-1} X. \tag{17}$$

This conditional-expectation formula gives the optimal forecast of $X_{(T+k)\Delta}$ when a discrete record over the finite past $[0, T\Delta]$, that is $X = (X_0, X_\Delta ..., X_{T\Delta})'$, is available in terms of minimizing the RMSE of the forecast.

In Formula (17), the s^{th} element of the row vector $\left(\gamma_{k\Delta}^{(0:T)}\right)' \Sigma_{0:T\Delta}^{-1}$ gives the weight of $X_{s\Delta}$ for $s = 0, 1, \ldots, T$. Figure 4 plots these weights, denoted by $w^*(s)$, when $H = 0.2$, $k\Delta = 1/50$, $T\Delta = 2$. It shows that the weight function $w^*(s)$ is U-shaped indicating that the initial observation X_0 is relatively important in forecasting $X_{(T+k)\Delta}$. Since the weights of IPϵA are always monotonically increasing regardless of the value of ϵ, this feature of the optimal weights suggests that the IPϵA forecasting formula is always sub-optimal.

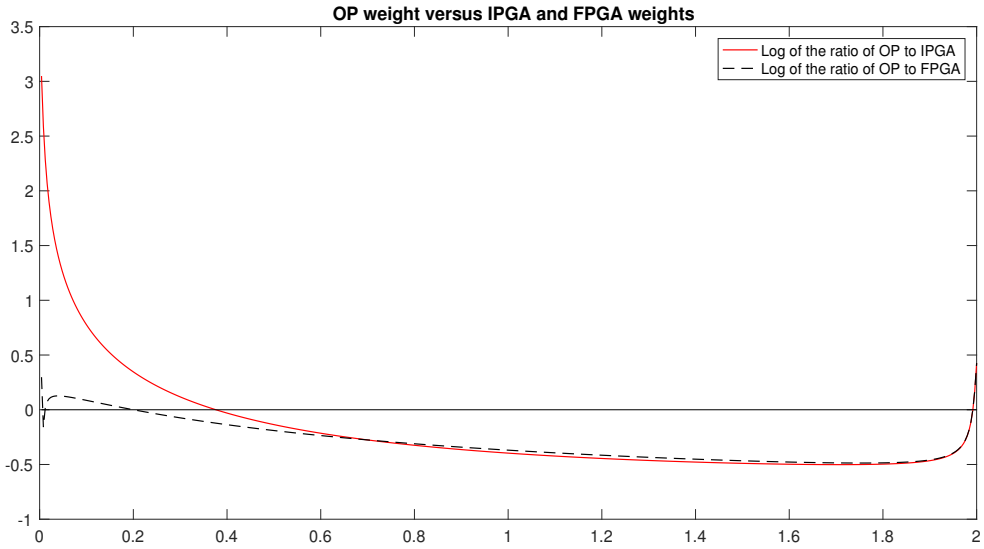

Figure 5: The log of the ratio of $w^*(s)$ to the normalized $\widetilde{w}_1(s)$ in IPGA and the log of the ratio of $w^*(s)$ to the normalized $w_2(s)$ in FPGA, both as functions of s for $H = 0.2$, $k\Delta = 1/50$, and $T\Delta = 2$.

Figure 5 plots the log of the ratio of $w^*(s)$ to the normalized $\widetilde{w}_1(s)$ (the weights used in IPGA) and the log of the ratio of $w^*(s)$ to the normalized $w_2(s)$ (the weights used in FPGA), for $s = 0, 1, \ldots, T$, when $H = 0.2$, $k\Delta = 1/50$, $T\Delta = 2$. It clearly shows that, compared to those adopted in the IPGA and FPGA formulas, the optimal weights $w^*(s)$ are significantly greater when s is close to 0 or the terminal point $T\Delta$, much lesser when s is away from the two ending points of the observation span. In other words, the optimal forecasting formula given in (17) places higher weights on the observations near the initial period and the latest period and lower weights on the observations in the middle. Also shown in the figure is that, compared to the FPGA formula, the IPGA formula applies the weights that are further away from the optimal ones given by $w^*(s)$.

3 Comparison based on Simulated Data

We now design Monte Carlo experiments to examine the performance of alternative forecasting formulas when a discrete and finite sample is simulated from the fBm. In all experiments, we set $\sigma = 1$, $H \in \{0.05, 0.1, 0.15, 0.2, 0.25, 0.4\}$, $\Delta = 1$, and assume

both σ and H are known.[7] As a result, no estimation is needed. The number of replications is 100,000 and used to calculate the RMSE. For each replication, we simulate 511 observations. The first 501 observations (hence $T = 501$) are used to generate forecasts. Alternative forecasting formulas are used to generate k-step-ahead forecasts with $k = 1, ..., 10$. The RMSEs from these forecasting formulas are reported in Tables 2-7. The last row in each table shows the theoretical RMSE of the optimal forecast, which is obtained as

$$RMSE^* = \sigma^2 + w^{*\prime}\Sigma_{0:T}w^* - 2w^{*\prime}\gamma_k^{(0:T)} = \sigma^2 - w^{*\prime}\Sigma_{0:T}w^*, \tag{18}$$

where $\sigma^2 = Var(X_{T+k})$ and $w^* = \Sigma_{0:T}^{-1}\gamma_k^{(0:T)}$.

The following conclusions can be drawn from the analysis of these tables. Firstly, it is evident that the optimal forecast (OP) consistently produces the lowest RMSE, which is also close to the theoretical RMSE. Secondly, as the value of k decreases, the performance improvement of OP over the other forecasting formulas becomes more significant. For instance, with H set to 0.25, OP improves upon IPGA by 5.14%, 3.47%, 2.76%, 2.48%, 2.23%, 2.05%, 1.89%, 1.81%, 1.70%, and 1.59% for k values ranging from 1 to 10, respectively.

Thirdly, as the value of H increases, the performance improvement of OP over the other forecasting formulas also becomes more substantial. For instance, with k set to 1, OP improves upon IPGA by 0.45%, 0.10%, 1.11%, 2.74%, 5.14%, and 16.17% for H values of 0.05, 0.1, 0.15, 0.2, 0.25, and 0.4, respectively. Fourthly, the relative performance of the four discretization schemes depends on the value of H. When H is small, such as $H = 0.05$, the scheme suggested by Gatheral et al. (2018) yields the smallest RMSE. However, as H increases, the middle scheme exhibits the best performance among the discretization-based methods.

Fifthly, except for the method proposed by Gatheral et al. (2018), the forecasting formulas based on finite-past records consistently yield smaller RMSEs compared to their infinite-past counterparts. However, the magnitude of this improvement is generally small. Lastly, it is worth noting that IPGA and its finite-past counterpart, FPGA, consistently outperform the other forecasting formulas when $H \leq 0.1$.

These findings provide valuable insights into the performance of the different forecasting methods and highlight the advantages of the optimal forecast (OP) over

[7]Due to the self-similarity property, by setting $\Delta = 1/250$ will not change the empirical results reported below.

other formulas in various scenarios.

Table 2: RMSE of the alternative methods for k-day-ahead forecasts when $H = 0.05$.

k	1	2	3	4	5	6	7	8	9	10
IPGA	0.7889	0.8055	0.8205	0.8288	0.8338	0.8419	0.8458	0.8519	0.8545	0.8577
IPRA	0.7919	0.8077	0.8222	0.8309	0.8357	0.8436	0.8472	0.8533	0.8559	0.8590
IPTA	0.7958	0.8093	0.8229	0.8317	0.8361	0.8437	0.8472	0.8533	0.8559	0.8589
IPMA	0.8035	0.8151	0.8277	0.8345	0.8387	0.8463	0.8497	0.8554	0.8578	0.8607
FPGA	0.7887	0.8052	0.8202	0.8285	0.8335	0.8415	0.8455	0.8516	0.8541	0.8572
FPRA	0.7916	0.8074	0.8219	0.8305	0.8353	0.8432	0.8468	0.8529	0.8554	0.8585
FPTA	0.7955	0.8090	0.8226	0.8314	0.8358	0.8434	0.8468	0.8529	0.8554	0.8585
FPMA	0.8031	0.8146	0.8273	0.8340	0.8382	0.8457	0.8491	0.8548	0.8572	0.8601
OP	0.7854	0.8028	0.8183	0.8271	0.8323	0.8403	0.8445	0.8507	0.8532	0.8564
Theoretical	0.7863	0.8044	0.8162	0.8250	0.8323	0.8384	0.8437	0.8485	0.8527	0.8566

Table 3: RMSE of the alternative methods for k-day-ahead forecasts when $H = 0.1$.

k	1	2	3	4	5	6	7	8	9	10
IPGA	0.8357	0.8772	0.9132	0.9367	0.9542	0.9678	0.9812	0.9935	1.0056	1.0136
IPRA	0.8396	0.8790	0.9146	0.9380	0.9550	0.9685	0.9818	0.9939	1.0059	1.0138
IPTA	0.8522	0.8872	0.9205	0.9431	0.9592	0.9719	0.9853	0.9969	1.0086	1.0162
IPMA	0.8406	0.8802	0.9155	0.9382	0.9554	0.9690	0.9818	0.9941	1.0062	1.0141
FPGA	0.8357	0.8773	0.9133	0.9367	0.9542	0.9678	0.9811	0.9934	1.0055	1.0134
FPRA	0.8396	0.8790	0.9144	0.9379	0.9548	0.9683	0.9816	0.9936	1.0056	1.0134
FPTA	0.8522	0.8871	0.9204	0.9430	0.9591	0.9718	0.9851	0.9967	1.0084	1.0159
FPMA	0.8404	0.8800	0.9153	0.9379	0.9552	0.9688	0.9815	0.9937	1.0058	1.0137
OP	0.8349	0.8765	0.9127	0.9362	0.9537	0.9674	0.9805	0.9928	1.0049	1.0128
Theoretical	0.8341	0.8819	0.9126	0.9357	0.9544	0.9702	0.9840	0.9962	1.0071	1.0171

4 Comparison based on Real Data

4.1 ML for fBm

Since $X \sim N(0, \Sigma_{0:T\Delta})$ with elements of $\Sigma_{0:T\Delta}$ being found from (1), the log likelihood function of X is,

$$\ln L(H, \sigma^2) = -\frac{\ln \sigma^2}{2} - \frac{1}{2\,(T+1)} \ln |\Sigma_{0:T\Delta}| - \frac{1}{2\,(T+1)\,\sigma^2} X' \Sigma_{0:T\Delta}^{-1} X. \tag{19}$$

When numerically maximizing $\ln L(H, \sigma^2)$, $|\Sigma_T|$ is calculated as the product of the eigenvalues of $\Sigma_{0:T\Delta}$.

Let $\hat{H}_{ML}$ and $\widehat{\sigma}^2_{ML}$ denote the maximum likelihood (ML) estimator of H and σ^2, respectively. The ML method is expected to deliver more efficient estimates than

Table 4: RMSE of the alternative methods for k-day-ahead forecasts when $H = 0.15$.

k	1	2	3	4	5	6	7	8	9	10
IPGA	0.8821	0.9651	1.0201	1.0569	1.093	1.1202	1.1443	1.1668	1.1870	1.2047
IPRA	0.8896	0.9673	1.0207	1.0567	1.0927	1.1196	1.1436	1.1659	1.1860	1.2036
IPTA	0.9135	0.9828	1.0330	1.0669	1.1018	1.1278	1.1511	1.1727	1.1920	1.2093
IPMA	0.8730	0.9595	1.0150	1.0524	1.0884	1.1159	1.1402	1.1628	1.1837	1.2014
FPGA	0.8823	0.9653	1.0202	1.0571	1.0931	1.1203	1.1444	1.1668	1.1870	1.2048
FPRA	0.8897	0.9673	1.0207	1.0567	1.0926	1.1195	1.1435	1.1657	1.1858	1.2034
FPTA	0.9136	0.9828	1.0330	1.0669	1.1018	1.1277	1.1510	1.1726	1.1918	1.2092
FPMA	0.8730	0.9594	1.0149	1.0523	1.0883	1.1158	1.1400	1.1627	1.1835	1.2011
OP	0.8724	0.9588	1.0144	1.0519	1.0880	1.1154	1.1397	1.1623	1.1831	1.2008
Theoretical	0.8725	0.9562	1.0105	1.0516	1.0850	1.1134	1.1382	1.1602	1.1801	1.1982

Table 5: RMSE of the alternative methods for k-day-ahead forecasts when $H = 0.2$.

k	1	2	3	4	5	6	7	8	9	10
IPGA	0.9297	1.0525	1.1336	1.1917	1.2414	1.2831	1.3232	1.3580	1.3885	1.4152
IPRA	0.9390	1.0549	1.1334	1.1903	1.2389	1.2806	1.3202	1.3550	1.3851	1.4117
IPTA	0.9728	1.0791	1.1533	1.2073	1.2539	1.2940	1.3325	1.3667	1.3961	1.4219
IPMA	0.9072	1.0355	1.1185	1.1781	1.2290	1.2717	1.3125	1.3475	1.3781	1.4055
FPGA	0.9299	1.0527	1.1338	1.1918	1.2416	1.2832	1.3234	1.3582	1.3886	1.4152
FPRA	0.9390	1.0549	1.1334	1.1902	1.2389	1.2805	1.3201	1.3549	1.3849	1.4115
FPTA	0.9728	1.0791	1.1533	1.2073	1.2539	1.2940	1.3324	1.3667	1.3960	1.4218
FPMA	0.9072	1.0355	1.1185	1.1781	1.2290	1.2716	1.3124	1.3474	1.3780	1.4053
OP	0.9049	1.0333	1.1161	1.1757	1.2267	1.2695	1.3103	1.3452	1.3755	1.4030
Theoretical	0.9049	1.0290	1.1109	1.1737	1.2252	1.2692	1.3079	1.3424	1.3737	1.4024

Table 6: RMSE of the alternative methods for k-day-ahead forecasts when $H = 0.25$.

k	1	2	3	4	5	6	7	8	9	10
IPGA	0.9840	1.1391	1.2451	1.3321	1.406	1.4658	1.515	1.5680	1.6171	1.6600
IPRA	0.9968	1.1418	1.2435	1.3285	1.4013	1.4601	1.5087	1.5612	1.6103	1.653
IPTA	1.0424	1.1755	1.2712	1.3529	1.4234	1.4804	1.5275	1.5790	1.6271	1.6688
IPMA	0.9442	1.1084	1.2187	1.3074	1.3829	1.4439	1.4942	1.5477	1.5977	1.6414
FPGA	0.9840	1.1391	1.2451	1.3321	1.4060	1.4658	1.5150	1.5680	1.6170	1.6600
FPRA	0.9967	1.1417	1.2434	1.3284	1.4012	1.4600	1.5086	1.5611	1.6101	1.6528
FPTA	1.0423	1.1755	1.2711	1.3529	1.4234	1.4803	1.5274	1.5789	1.6269	1.6687
FPMA	0.9441	1.1084	1.2187	1.3074	1.3828	1.4438	1.4941	1.5477	1.5975	1.6412
OP	0.9359	1.1009	1.2116	1.2999	1.3753	1.4363	1.4869	1.5402	1.5900	1.6341
Theoretical	0.9325	1.1006	1.2140	1.3021	1.3751	1.4381	1.4937	1.5436	1.5892	1.6312

Table 7: RMSE of the alternative methods for k-day-ahead forecasts when $H = 0.4$.

k	1	2	3	4	5	6	7	8	9	10
IPGA	1.1479	1.4517	1.6781	1.8627	2.0197	2.1581	2.2828	2.4005	2.5032	2.6046
IPRA	1.1736	1.4561	1.6726	1.8509	2.0037	2.1390	2.2610	2.3770	2.4782	2.5783
IPTA	1.2588	1.5265	1.7351	1.9087	2.0578	2.1906	2.3106	2.4248	2.5244	2.6234
IPMA	1.0410	1.3591	1.5922	1.7799	1.9396	2.0795	2.2054	2.3246	2.4285	2.5305
FPGA	1.1470	1.4507	1.6769	1.8615	2.0184	2.1568	2.2814	2.3991	2.5016	2.6030
FPRA	1.1731	1.4555	1.6719	1.8501	2.0029	2.1381	2.2600	2.3760	2.4771	2.5772
FPTA	1.2582	1.5258	1.7343	1.9078	2.0568	2.1896	2.3095	2.4236	2.5231	2.6221
FPMA	1.0407	1.3587	1.5917	1.7793	1.9390	2.0788	2.2047	2.3238	2.4276	2.5296
OP	0.9881	1.3022	1.5332	1.7181	1.8768	2.0148	2.1395	2.2581	2.3622	2.4631
Theoretical	0.9881	1.3020	1.5304	1.7165	1.8764	2.0181	2.1462	2.2638	2.3729	2.4749

method-of-moment (MM), the latter of which was proposed in Lang and Roueff (2001), Barndorff-Nielsen et al. (2013), Brouste et al. (2020), and Wang et al. (2023), although MM is computationally cheaper to implement. It is also expected to be more efficient than the maximum composite likelihood method of Bennedsen et al. (2022) although the latter method is applicable to more complicated models.

4.2 Results

We now examine the performance of alternative forecasting formulas based on real data. We download daily RV time series of the S&P 500 market ETF (SPY) and nine industry ETFs from the Risk Lab constructed by Dacheng Xiu.[8] The sample period is from October 1, 2017 to September 30, 2022. Following Gatheral et al. (2018), we model the log of each RV time series by a scaled fBm $X(t) = \sigma B^H(t)$. The ML method is then applied to estimate H and σ^2. A two-year rolling window is used to fit the model and generate the ML estimates, and then calculate k-day-ahead forecasts of log RV with $k = 1, 2, ..., 10$. The averaged RMSE of these forecasts are hence obtained with the data from October 1, 2019 to September 30, 2022. We set $\Delta = 1/252$ in this exercise to reflect 252 trading days in a year.

In Figure 6, the top panel plots the full sample of log RV of SPY. The bottom panel reports the rolling window estimates of H. These estimates fluctuate within the interval $[0.2, 0.3]$ and are much lower than 0.5, indicating roughness.

Table 8 reports the RMSEs of the alternative forecasting formulas for k-day-ahead forecasts of log RV of SPY with $k = 1, 2, ..., 10$. It can be seen that OP always yields the lowest RMSE. The smaller the k is, the bigger its improvement over other

[8] See https://dachxiu.chicagobooth.edu/#risklab.

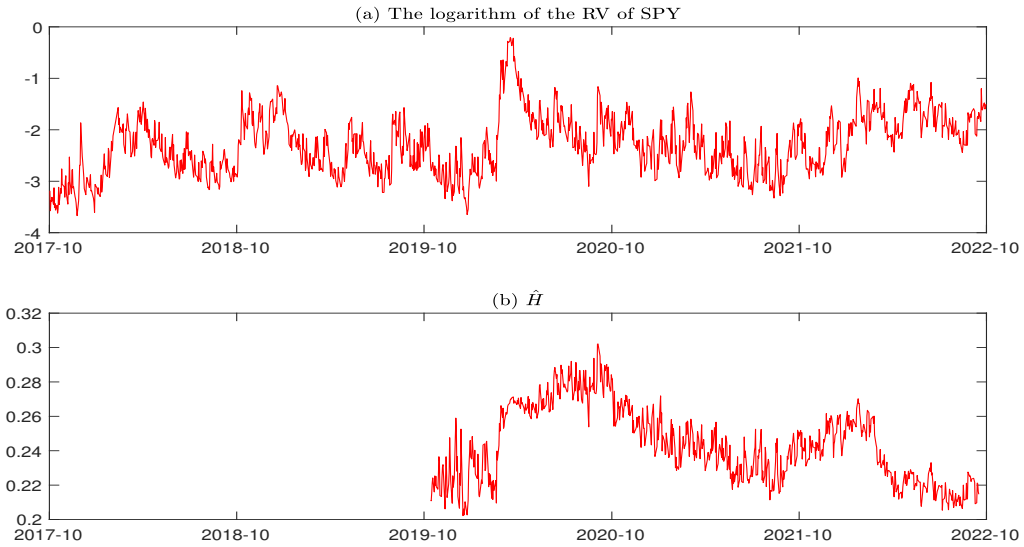

Figure 6: (a) The log RV of SPY between October 1, 2017 and September 30, 2022; (b) Rolling window estimates of H for log RV of SPY.

forecasting formulas. For example, it improves upon IPGA (i.e. the method used by Gatheral et al., 2018) by 4.85%, 2.84%, 1.48%, 1.29%, 1.53%, 1.06%, 1.07%, 1.38%, 1.37%, 1.40% for $k = 1, ..., 10$, respectively. The magnitude of these improvements is consistent with our findings based on simulated data. Judged by the forecast results provided in the literature (Andersen et al. 2003, Gatheral et al. 2018, Wang et al. 2023), 4.85% for 1-day-ahead forecasts is large and economically significant. The outperformance of OP over IPGA and FPGA have been explained in Figure 5. Both IPGA and FPGA put too less weight on X_s when s is near 0 and near $T\Delta$. It can also be found from the table is that the second best method is FPMA, followed closely by IPMA. The finite-past methods always perform slightly better than the infinite-past methods except for the adjustment suggested by Gatheral et al. (2018). All these empirical findings are consistent with the findings obtained from the simulated data.

Figure 7 plots the rolling window estimates of H for the log RV series of the nine industry ETFs. These estimates suggest that the estimates are fluctuating within the interval $[0.1, 0.35]$. These values are lower than 0.5, indicating roughness.

Tables 9-17 report the RMSEs of the alternative forecasting formulas for k-day-ahead forecasts of log RV of the nine industry ETFs with $k = 1, 2, ..., 10$. It can

Table 8: RMSE of the alternative methods for k-day-ahead forecasts of log RV of SPY between October 1, 2017 and September 30, 2022. Boldface corresponds to the lowest RMSE.

k	1	2	3	4	5	6	7	8	9	10
IPGA	0.2897	0.3372	0.3711	0.3933	0.4109	0.4285	0.4427	0.4542	0.4667	0.4776
IPRA	0.2951	0.3406	0.3721	0.3932	0.4115	0.4285	0.4421	0.4540	0.4664	0.4778
IPTA	0.3089	0.3508	0.3791	0.3990	0.4176	0.4334	0.4464	0.4587	0.4706	0.4822
IPMA	0.2783	0.3292	0.3659	0.3887	0.4059	0.4245	0.4390	0.4500	0.4629	0.4737
FPGA	0.2896	0.3371	0.3710	0.3932	0.4108	0.4283	0.4425	0.4540	0.4664	0.4773
FPRA	0.2950	0.3405	0.3721	0.3931	0.4114	0.4284	0.4419	0.4538	0.4662	0.4776
FPTA	0.3088	0.3507	0.3790	0.3989	0.4174	0.4332	0.4462	0.4584	0.4703	0.4819
FPMA	0.2783	0.3292	0.3659	0.3886	0.4058	0.4244	0.4388	0.4498	0.4626	0.4735
OP	**0.2763**	**0.3279**	**0.3657**	**0.3883**	**0.4047**	**0.4240**	**0.4380**	**0.4480**	**0.4604**	**0.4710**

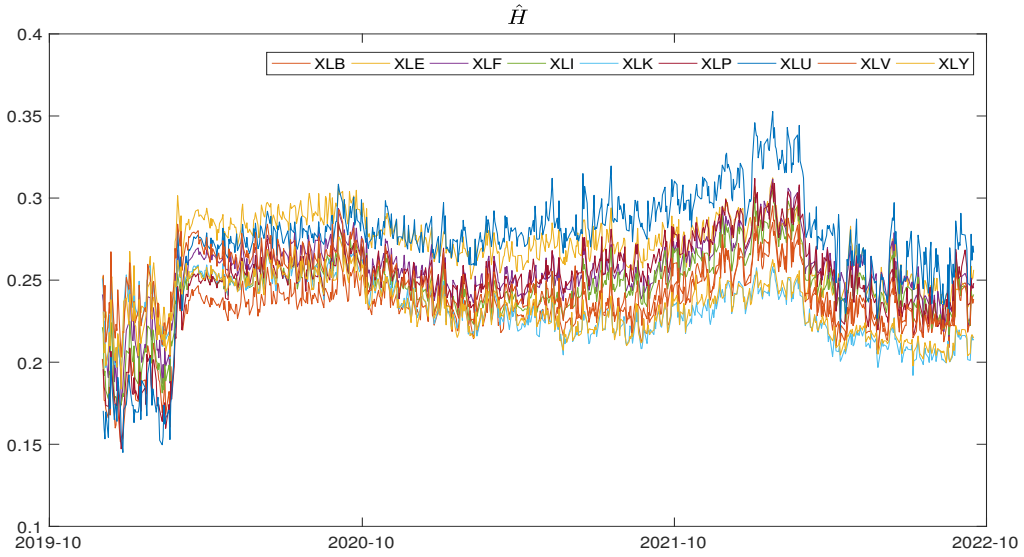

Figure 7: Rolling window estimates of H for log RV of 9 industry ETFs.

be seen that OP always yields the lowest RMSE.[9] For example, when $k = 1$, its improvement upon IPGA is 5.80%, 7.09%, 6.78%, 6.77%, 4.11%, 7.70%, 9.71%, 5.72%, 4.32% for the nine industry ETFs, respectively. These improvements are large and economically significant. Again, both IPGA and FPGA perform relatively poorly. Moreover, the second best methods are FPMA and IPMA.

We also examine the mean absolute forecast errors (MAEs) of the alternative forecasting formulas for k-day-ahead forecasts of log RV of the SPY and the nine industry ETFs as well as the simulated data used before with $k = 1, 2, ..., 10$ in the Appendix B. Theoretically the OP is the optimal forecast in terms of RMSE, its performance under the MAE is also remarkable. For $k = 1$, the improvement over the IPGA method is 6.43%, 5.69%, 4.77%, 5.67%, 7.01%, 4.50%, 5.91%, 7.52%, 6.76% and 5.02% for the SPY and nine industry ETFs, respectively.

To understand whether or not the forecasts produced by the OP method is statistically indifferent from those from IPGA for k-day-ahead forecast, Table 18 reports the p-value of Diebold and Mariano (DM) statistic with $k = 1, ..., 10$ for the SPY ETF and the nine industry ETFs (Diebold and Mariano, 1995). The DM test is a method for testing for the equal accuracy of two competing forecasts (i.e. IPGA and OP in our case). When $k = 1$, we always reject the null hypothesis that the two methods generate the equally accurate forecasts at the 1% level. When $k = 2$, we reject the null hypothesis that the two methods generate the equally accurate forecasts at the 10% level in eight out of ten cases. For larger values of k, we cannot reject the null hypothesis at any conventional levels of significance.

Table 9: RMSE of the alternative methods for k-day-ahead forecasts of XLB. Boldface corresponds to the lowest RMSE.

k	1	2	3	4	5	6	7	8	9	10
IPGA	0.2188	0.2555	0.2828	0.3016	0.3175	0.3319	0.3421	0.3513	0.3602	0.3691
IPRA	0.2220	0.2575	0.2833	0.3018	0.3180	0.3315	0.3415	0.3507	0.3596	0.3687
IPTA	0.2327	0.2657	0.2893	0.3071	0.3229	0.3350	0.3449	0.3542	0.3631	0.3721
IPMA	0.2090	0.2481	0.2774	0.2968	0.3133	0.3289	0.3390	0.3480	0.3567	0.3657
FPGA	0.2188	0.2555	0.2828	0.3016	0.3175	0.3320	0.3422	0.3514	0.3603	0.3692
FPRA	0.2220	0.2575	0.2833	0.3018	0.3180	0.3316	0.3416	0.3508	0.3597	0.3687
FPTA	0.2327	0.2657	0.2893	0.3071	0.3229	0.3351	0.3450	0.3542	0.3632	0.3722
FPMA	0.2090	0.2481	0.2775	0.2969	0.3133	0.3290	0.3390	0.3480	0.3568	0.3658
OP	**0.2068**	**0.2460**	**0.2760**	**0.2955**	**0.3121**	**0.3283**	**0.3377**	**0.3462**	**0.3542**	**0.3631**

[9]The only exception is for XLK when $k = 3, 4$. One possible explanation for this result is that there may exist model mis-specification for this particular RV series.

Table 10: RMSE of the alternative methods for k-day-ahead forecasts of XLE. Boldface corresponds to the lowest RMSE.

k	1	2	3	4	5	6	7	8	9	10
IPGA	0.1812	0.2157	0.2398	0.2581	0.2716	0.2839	0.294	0.3033	0.3128	0.3224
IPRA	0.1849	0.2174	0.2406	0.2577	0.2711	0.2829	0.2927	0.3022	0.3119	0.3214
IPTA	0.1948	0.2247	0.2464	0.2622	0.2754	0.2866	0.2964	0.3060	0.3158	0.3250
IPMA	0.1717	0.2088	0.2343	0.2537	0.2672	0.2798	0.2898	0.2988	0.3082	0.3182
FPGA	0.1812	0.2157	0.2398	0.2580	0.2716	0.2839	0.2940	0.3034	0.3128	0.3225
FPRA	0.1848	0.2173	0.2405	0.2577	0.2711	0.2829	0.2927	0.3022	0.3119	0.3215
FPTA	0.1948	0.2246	0.2464	0.2622	0.2754	0.2866	0.2964	0.3060	0.3158	0.3250
FPMA	0.1717	0.2088	0.2343	0.2537	0.2672	0.2798	0.2898	0.2989	0.3083	0.3183
OP	**0.1692**	**0.2067**	**0.2328**	**0.2528**	**0.2659**	**0.2783**	**0.2875**	**0.2957**	**0.3045**	**0.3147**

Table 11: RMSE of the alternative methods for k-day-ahead forecasts of XLF. Boldface corresponds to the lowest RMSE.

k	1	2	3	4	5	6	7	8	9	10
IPGA	0.2127	0.2511	0.2797	0.2993	0.3152	0.3297	0.3428	0.354	0.3638	0.3741
IPRA	0.2165	0.2532	0.2801	0.2989	0.3148	0.3293	0.3422	0.3533	0.3633	0.3736
IPTA	0.2277	0.2618	0.2864	0.3043	0.3200	0.3341	0.3464	0.3573	0.3674	0.3775
IPMA	0.2021	0.2430	0.2738	0.2941	0.3100	0.3250	0.3386	0.3498	0.3596	0.3700
FPGA	0.2127	0.2511	0.2797	0.2993	0.3152	0.3298	0.3429	0.3540	0.3639	0.3741
FPRA	0.2165	0.2532	0.2801	0.2989	0.3148	0.3294	0.3422	0.3533	0.3634	0.3737
FPTA	0.2277	0.2618	0.2864	0.3043	0.3200	0.3341	0.3464	0.3573	0.3674	0.3775
FPMA	0.2021	0.2430	0.2738	0.2941	0.3100	0.3250	0.3386	0.3499	0.3596	0.3701
OP	**0.1992**	**0.2404**	**0.2721**	**0.2923**	**0.308**	**0.3232**	**0.3365**	**0.3474**	**0.3565**	**0.367**

Table 12: RMSE of the alternative methods for k-day-ahead forecasts of XLI. Boldface corresponds to the lowest RMSE.

k	1	2	3	4	5	6	7	8	9	10
IPGA	0.2223	0.2612	0.2921	0.3135	0.3305	0.3460	0.3578	0.3687	0.3787	0.3887
IPRA	0.2254	0.2634	0.2928	0.3136	0.3308	0.3456	0.3573	0.3683	0.3784	0.3883
IPTA	0.2369	0.2728	0.2998	0.3193	0.3362	0.3497	0.3613	0.3722	0.3823	0.3918
IPMA	0.2111	0.2521	0.2856	0.3082	0.3255	0.3423	0.3540	0.3649	0.3748	0.3852
FPGA	0.2223	0.2612	0.2921	0.3136	0.3305	0.3461	0.3579	0.3688	0.3788	0.3888
FPRA	0.2254	0.2634	0.2929	0.3136	0.3309	0.3457	0.3574	0.3684	0.3785	0.3884
FPTA	0.2369	0.2729	0.2998	0.3193	0.3362	0.3498	0.3614	0.3723	0.3824	0.3919
FPMA	0.2111	0.2521	0.2856	0.3082	0.3256	0.3423	0.3541	0.3650	0.3749	0.3853
OP	**0.2082**	**0.2492**	**0.2839**	**0.3067**	**0.3242**	**0.3415**	**0.3527**	**0.3632**	**0.3726**	**0.3829**

Table 13: RMSE of the alternative methods for k-day-ahead forecasts of XLK. Boldface corresponds to the lowest RMSE.

k	1	2	3	4	5	6	7	8	9	10
IPGA	0.2581	0.2982	0.3272	0.3446	0.3576	0.3710	0.3821	0.3918	0.4009	0.4099
IPRA	0.2632	0.3016	0.3282	0.3444	0.3578	0.3709	0.3815	0.3914	0.4004	0.4097
IPTA	0.2749	0.3100	0.3335	0.3486	0.3622	0.3746	0.3849	0.3951	0.4040	0.4133
IPMA	0.2492	0.2924	**0.3241**	**0.3419**	0.3544	0.3683	0.3794	0.3886	0.3977	0.4066
FPGA	0.2581	0.2982	0.3272	0.3447	0.3577	0.3711	0.3822	0.3919	0.4010	0.4101
FPRA	0.2632	0.3016	0.3283	0.3445	0.3579	0.3709	0.3816	0.3915	0.4005	0.4098
FPTA	0.2749	0.3100	0.3335	0.3486	0.3623	0.3747	0.3850	0.3952	0.4041	0.4134
FPMA	0.2492	0.2924	**0.3241**	0.3420	0.3544	0.3683	0.3795	0.3887	0.3978	0.4067
OP	**0.2479**	**0.2919**	0.3246	0.3422	**0.3541**	**0.3681**	**0.3786**	**0.387**	**0.3954**	**0.4042**

Table 14: RMSE of the alternative methods for k-day-ahead forecasts of XLP. Boldface corresponds to the lowest RMSE.

k	1	2	3	4	5	6	7	8	9	10
IPGA	0.2141	0.2533	0.2834	0.3052	0.3237	0.3417	0.3552	0.3686	0.3805	0.3927
IPRA	0.2163	0.2542	0.2828	0.3042	0.3234	0.3405	0.3544	0.3677	0.3800	0.3928
IPTA	0.2277	0.2635	0.2903	0.3109	0.3299	0.3457	0.3597	0.3724	0.3848	0.3972
IPMA	0.2021	0.2433	0.2753	0.2978	0.3166	0.3360	0.3494	0.3634	0.3753	0.3882
FPGA	0.2141	0.2533	0.2834	0.3052	0.3238	0.3417	0.3552	0.3686	0.3805	0.3928
FPRA	0.2163	0.2542	0.2828	0.3042	0.3234	0.3405	0.3544	0.3677	0.3801	0.3928
FPTA	0.2277	0.2635	0.2903	0.3109	0.3299	0.3457	0.3597	0.3725	0.3848	0.3973
FPMA	0.2021	0.2433	0.2753	0.2978	0.3166	0.3361	0.3494	0.3634	0.3754	0.3882
OP	**0.1988**	**0.2397**	**0.2722**	**0.2947**	**0.3134**	**0.3336**	**0.3464**	**0.3605**	**0.3720**	**0.3854**

Table 15: RMSE of the alternative methods for k-day-ahead forecasts of XLU. Boldface corresponds to the lowest RMSE.

k	1	2	3	4	5	6	7	8	9	10
IPGA	0.1807	0.2162	0.2442	0.2660	0.2839	0.2997	0.3140	0.3275	0.3395	0.3513
IPRA	0.1822	0.2167	0.2437	0.2652	0.2828	0.2986	0.3131	0.3266	0.3389	0.3509
IPTA	0.1926	0.2255	0.2512	0.2718	0.2886	0.3041	0.3183	0.3313	0.3435	0.3552
IPMA	0.1689	0.2059	0.2355	0.2582	0.2769	0.2931	0.3079	0.3220	0.3343	0.3465
FPGA	0.1806	0.2162	0.2442	0.2659	0.2839	0.2997	0.3140	0.3275	0.3395	0.3512
FPRA	0.1822	0.2166	0.2437	0.2651	0.2828	0.2986	0.3131	0.3265	0.3388	0.3508
FPTA	0.1926	0.2255	0.2512	0.2718	0.2886	0.3041	0.3183	0.3313	0.3434	0.3551
FPMA	0.1689	0.2059	0.2355	0.2582	0.2769	0.2931	0.3079	0.3220	0.3342	0.3465
OP	**0.1647**	**0.2012**	**0.2313**	**0.2544**	**0.2734**	**0.2895**	**0.3042**	**0.3185**	**0.3304**	**0.3429**

Table 16: RMSE of the alternative methods for k-day-ahead forecasts of XLV. Boldface corresponds to the lowest RMSE.

k	1	2	3	4	5	6	7	8	9	10
IPGA	0.2126	0.2490	0.2764	0.2954	0.3108	0.3263	0.3375	0.3476	0.3573	0.3671
IPRA	0.2160	0.2511	0.2772	0.2955	0.3115	0.3262	0.3373	0.3474	0.3573	0.3673
IPTA	0.2264	0.2593	0.2834	0.3007	0.3167	0.3300	0.3410	0.3509	0.3609	0.3707
IPMA	0.2033	0.2416	0.2709	0.2907	0.3061	0.3228	0.3340	0.3443	0.3539	0.3639
FPGA	0.2126	0.2490	0.2764	0.2954	0.3108	0.3263	0.3375	0.3477	0.3574	0.3672
FPRA	0.2159	0.2511	0.2772	0.2955	0.3115	0.3262	0.3373	0.3474	0.3573	0.3673
FPTA	0.2264	0.2593	0.2834	0.3007	0.3167	0.3301	0.3410	0.3510	0.3609	0.3707
FPMA	0.2033	0.2416	0.2709	0.2907	0.3061	0.3228	0.3340	0.3443	0.3539	0.3639
OP	**0.2011**	**0.2392**	**0.2692**	**0.2890**	**0.3042**	**0.3217**	**0.3325**	**0.3424**	**0.3515**	**0.3615**

Table 17: RMSE of the alternative methods for k-day-ahead forecasts of XLY. Boldface corresponds to the lowest RMSE.

k	1	2	3	4	5	6	7	8	9	10
IPGA	0.2560	0.2966	0.325	0.3427	0.3579	0.3729	0.3842	0.3936	0.4026	0.4125
IPRA	0.2605	0.2992	0.3253	0.3425	0.3581	0.3724	0.3832	0.3922	0.4013	0.4118
IPTA	0.2721	0.3075	0.3309	0.3475	0.3631	0.3763	0.3867	0.3957	0.4052	0.4161
IPMA	0.2469	0.2903	0.3210	0.3386	0.3537	0.3696	0.3809	0.3900	0.3983	0.4079
FPGA	0.2560	0.2966	0.3250	0.3428	0.3580	0.3730	0.3843	0.3938	0.4028	0.4127
FPRA	0.2605	0.2992	0.3253	0.3425	0.3581	0.3724	0.3832	0.3923	0.4014	0.4119
FPTA	0.2721	0.3075	0.3309	0.3475	0.3631	0.3763	0.3868	0.3958	0.4054	0.4162
FPMA	0.2469	0.2903	0.3210	0.3387	0.3537	0.3697	0.3810	0.3901	0.3984	0.4081
OP	**0.2454**	**0.2893**	**0.3205**	**0.3377**	**0.3522**	**0.3685**	**0.3791**	**0.3873**	**0.3945**	**0.4038**

Table 18: P-value of DM test for IPGA and OP for k-day-ahead forecasts of log RV.

k	1	2	3	4	5	6	7	8	9	10
SPY	0.0003	0.0941	0.4347	0.5373	0.5057	0.6682	0.6851	0.6233	0.6424	0.6422
XLB	0.0003	0.0617	0.2804	0.4108	0.5323	0.7054	0.6808	0.6594	0.6373	0.6420
XLE	0.0004	0.0853	0.2954	0.5111	0.5569	0.6238	0.6111	0.5759	0.5754	0.6125
XLF	0.0001	0.0552	0.3052	0.4262	0.4862	0.5794	0.6288	0.6369	0.6266	0.6491
XLI	0.0000	0.0239	0.2218	0.3860	0.4924	0.6611	0.6586	0.6520	0.6483	0.6729
XLK	0.0024	0.1928	0.6661	0.7272	0.6489	0.7383	0.7205	0.6500	0.6341	0.6365
XLP	0.0001	0.0367	0.1802	0.2882	0.3698	0.5238	0.5367	0.5805	0.5868	0.6310
XLU	0.0000	0.0204	0.1334	0.2789	0.4045	0.4798	0.5331	0.5796	0.5929	0.6268
XLV	0.0008	0.0728	0.3083	0.4379	0.4965	0.6811	0.6925	0.6958	0.6825	0.7041
XLY	0.0015	0.1319	0.4774	0.4999	0.5170	0.6597	0.6529	0.5989	0.5329	0.5157

4.3 Additional empirical results

The empirical study reported earlier is based on the sample period from October 1, 2017 to September 30, 2022. It is well known that the sample period contains the financial crash in 2020 that began on February 20, 2020, and ended on April 7, 2020. This crash may explain why the estimated H in the bottom panel of Figure 6 moved up from its values from the near 0.2 level in February 2020 to the near 0.3 level in April 2020.

To check the robustness of the empirical results reported earlier, we now examine the performance of alternative forecasting formulas based on the daily RV time series of SPY from January 2, 2012 to December 31, 2019. Once again, we model the log of each RV time series by fBm and use the ML method to estimate H and σ^2. A six-year rolling window is used to fit fBm and based on the ML estimates of H and σ^2 in fBm, we obtain k-day-ahead forecasts of log RV with $k = 1, 2, ..., 10$ for the remaining two years.

The top panel of Figure 8 plots the full sample of log RV of SPY. The bottom panel plots the rolling window estimates of H. These estimates fluctuate within the much narrower interval $[0.19, 0.22]$ than before and are much lower than 0.5, indicating roughness.

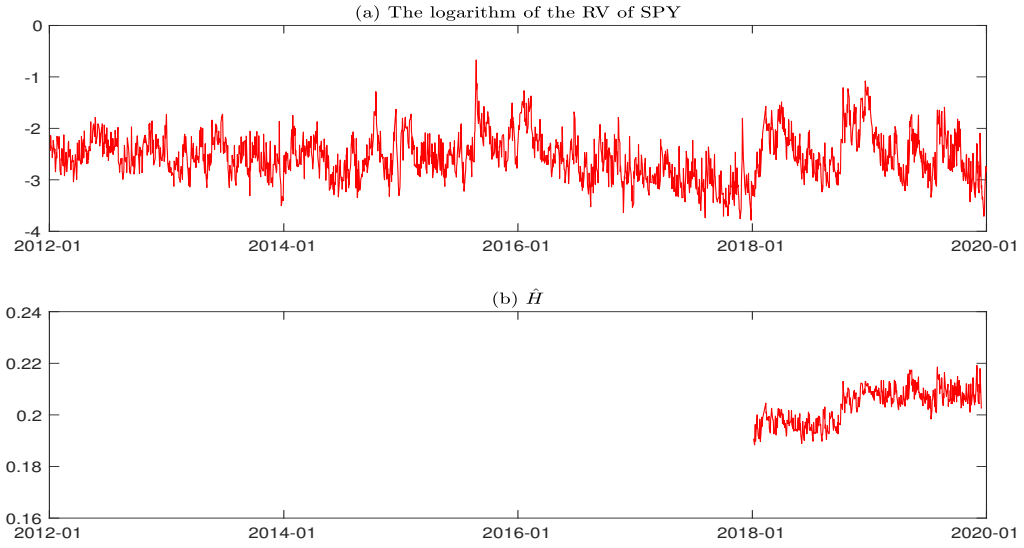

Figure 8: (a) The log RV of SPY between January 2, 2012 and December 31, 2019; (b) Rolling window estimates of H for log RV of SPY.

Table 19 reports the RMSEs of the alternative forecasting formulas for k-day-ahead forecasts of log RV of SPY with $k = 1, ..., 10$. It can be seen that OP continues to yield the lowest RMSE always. The smaller the k is, the bigger its improvement over other forecasting formulas. For example, it improves upon IPGA by 3.56%, 2.20%, 2.19%, 2.15%, 1.74%, 1.54%, 1.30%, 1.33%, 1.35%, 1.09% for $k = 1, ..., 10$, respectively. The magnitude of these improvements is consistent with our findings based on simulated data and the sample between October 1, 2017 and September 30, 2022. This finding suggests that our empirical results are not driven by the 2020 financial crash.

To understand whether or not the OP and IPGA methods generate statistically equally accurate forecasts, Table 20 reports the p-value of DM statistic with $k = 1, ..., 10$ for SPY between January 2, 2012 and December 31, 2019. When $k = 1$, we reject the null hypothesis that the two methods generate the equally accurate forecasts at the 1% level. When $k = 2, 3$, we reject the null hypothesis that the two methods generate the equally accurate forecasts at the 10% level. For larger values of k, we cannot reject the null hypothesis at any conventional levels of significance.

Table 19: RMSE of the alternative methods for k-day-ahead forecasts of log RV of SPY between January 2, 2012 and December 31, 2019. Boldface corresponds to the lowest RMSE.

k	1	2	3	4	5	6	7	8	9	10
IPGA	0.2854	0.3254	0.3505	0.3710	0.3913	0.4084	0.4223	0.4332	0.4429	0.4534
IPRA	0.2887	0.3252	0.3497	0.3705	0.3904	0.4077	0.4211	0.4319	0.4421	0.4525
IPTA	0.3001	0.3327	0.3563	0.3769	0.3958	0.4127	0.4253	0.4359	0.4463	0.4561
IPMA	0.2768	0.3195	0.3446	0.3650	0.3862	0.4037	0.4183	0.4292	0.4387	0.4499
FPGA	0.2853	0.3254	0.3505	0.3709	0.3912	0.4083	0.4222	0.4331	0.4427	0.4532
FPRA	0.2887	0.3252	0.3496	0.3704	0.3903	0.4076	0.4210	0.4318	0.4419	0.4523
FPTA	0.3001	0.3326	0.3563	0.3768	0.3957	0.4126	0.4251	0.4358	0.4462	0.4559
FPMA	0.2768	0.3195	0.3446	0.3649	0.3861	0.4036	0.4182	0.4290	0.4385	0.4497
OP	**0.2756**	**0.3184**	**0.3430**	**0.3632**	**0.3846**	**0.4022**	**0.4169**	**0.4275**	**0.4370**	**0.4485**

Table 20: P-value of DM test to compare k-day-ahead forecasts of log RV of SPY between January 2, 2012 and December 31, 2019 from IPGA and OP.

k	1	2	3	4	5	6	7	8	9	10
SPY	0.0031	0.0879	0.0914	0.1322	0.2171	0.2675	0.3596	0.3646	0.3749	0.4773

5 Conclusion

In this study, we have investigated the performance of alternative forecasting formulas with fractional Brownian motion in a discrete and finite sample context. Existing literature has derived two optimal forecasting formulas, based on continuous records, which differ in their treatment of the past information: one with an infinite past and the other with a finite past. When only discrete and finite past data are available, these forecasting formulas can be discretized using various methods, resulting in two distinct classes of discretization-based formulas.

Alternatively, instead of discretizing these forecasting formulas, one can directly employ the conditional expectation method to generate optimal forecasts based on the discrete and finite past sample. The conditional expectation approach optimizes the forecast accuracy by minimizing the RMSE.

Through extensive analysis using simulated data and real RV data, we consistently find that the conditional expectation outperforms both classes of discretization-based forecasting formulas across all considered forecast horizons. The improvement in accuracy becomes more significant as the forecast horizon shortens. For instance, when the forecast horizon is one day, the conditional expectation approach achieves an approximate 5% enhancement over the currently implemented forecasting formula in the literature. This improvement is not only statistically significant but also economically meaningful.

Our findings underscore the superiority of the conditional expectation method in forecasting accuracy compared to the discretization-based formulas employed in the current literature. These results contribute to advancing our understanding of forecasting performance in the context of fractional Brownian motion.

A Proof of Proposition 2.1

Proof of Proposition 2.1. Without loss of generality, let us assume $k = 1$. In this case, the weight function becomes

$$\omega_1(s) = \frac{\cos(H\pi)}{\pi} \frac{1}{(T-s+1)(T-s)^{H+0.5}}$$

We then have

$$\begin{aligned}
\int_{-\infty}^{T} \omega_1(s)\, ds &= \frac{\cos(H\pi)}{\pi} \int_{-\infty}^{T} \frac{1}{(T-s+1)(T-s)^{H+0.5}} ds \\
&= \frac{\cos(H\pi)}{\pi} \int_{0}^{\infty} \frac{1}{(1+u)u^{H+0.5}} du \\
&= \frac{\cos(H\pi)}{\pi} \pi \csc((H+0.5)\pi) \\
&= \frac{\cos(H\pi)}{\sin(H\pi+0.5\pi)} \\
&= \frac{\cos(H\pi)}{\sin(0.5\pi)\cos(H\pi)+\cos(0.5\pi)\sin(H\pi)} \\
&= 1.
\end{aligned}$$

where $\csc((H+0.5)\pi) := 1/\sin((H+0.5)\pi)$ and the third equation comes from the Formula 361 on Page 290 of Tallarida (2015).

B Model evaluation in terms of MAE

B.1 Simulation

Table 21: MAE of the alternative methods for k-day-ahead forecasts when $H = 0.05$.

k	1	2	3	4	5	6	7	8	9	10
IPGA	0.6301	0.6434	0.6541	0.6619	0.6661	0.6711	0.6749	0.6796	0.6812	0.6841
IPRA	0.6321	0.6450	0.6557	0.6635	0.6676	0.6727	0.6760	0.6807	0.6821	0.6852
IPTA	0.6350	0.6462	0.6563	0.6641	0.6679	0.6730	0.6761	0.6807	0.6822	0.6850
IPMA	0.6419	0.6511	0.6600	0.6664	0.6700	0.6744	0.6780	0.6822	0.6836	0.6867
FPGA	0.6299	0.6432	0.6540	0.6617	0.6658	0.6708	0.6747	0.6793	0.6809	0.6837
FPRA	0.6319	0.6448	0.6554	0.6632	0.6673	0.6723	0.6757	0.6803	0.6818	0.6848
FPTA	0.6348	0.6460	0.6561	0.6638	0.6677	0.6727	0.6758	0.6805	0.6819	0.6846
FPMA	0.6415	0.6507	0.6597	0.6660	0.6695	0.6740	0.6776	0.6818	0.6832	0.6861
OP	0.6271	0.6411	0.6524	0.6605	0.6648	0.6698	0.6739	0.6787	0.6803	0.6829

B.2 Empirical studies

Table 22: MAE of the alternative methods for k-day-ahead forecasts when $H = 0.1$.

k	1	2	3	4	5	6	7	8	9	10
IPGA	0.6672	0.7004	0.7287	0.7467	0.7622	0.7717	0.7827	0.7928	0.8024	0.8092
IPRA	0.6705	0.7018	0.7296	0.7478	0.7627	0.7721	0.7832	0.7931	0.8028	0.8093
IPTA	0.6806	0.7082	0.7343	0.7518	0.7659	0.7750	0.7861	0.7954	0.8050	0.8111
IPMA	0.6710	0.7031	0.7307	0.7480	0.7632	0.7724	0.7831	0.7932	0.8029	0.8096
FPGA	0.6673	0.7005	0.7287	0.7467	0.7621	0.7718	0.7826	0.7928	0.8023	0.8091
FPRA	0.6704	0.7017	0.7295	0.7477	0.7626	0.7720	0.7830	0.7929	0.8026	0.8090
FPTA	0.6805	0.7081	0.7342	0.7516	0.7658	0.7749	0.7860	0.7953	0.8048	0.8109
FPMA	0.6709	0.7029	0.7305	0.7478	0.7630	0.7722	0.7828	0.7930	0.8026	0.8093
OP	0.6666	0.6998	0.7283	0.7464	0.7617	0.7713	0.7821	0.7923	0.8020	0.8087

Table 23: MAE of the alternative methods for k-day-ahead forecasts when $H = 0.15$.

k	1	2	3	4	5	6	7	8	9	10
IPGA	0.7037	0.7695	0.8152	0.8432	0.8729	0.8946	0.9124	0.9306	0.9481	0.9632
IPRA	0.7094	0.7715	0.8159	0.8433	0.8727	0.8942	0.9118	0.9302	0.9473	0.9622
IPTA	0.7284	0.7838	0.8257	0.8515	0.8800	0.9006	0.9177	0.9356	0.9520	0.9666
IPMA	0.6970	0.7652	0.811	0.8396	0.8693	0.8912	0.9092	0.9278	0.9455	0.9604
FPGA	0.7039	0.7696	0.8154	0.8434	0.8730	0.8946	0.9124	0.9307	0.9480	0.9632
FPRA	0.7095	0.7715	0.8159	0.8433	0.8727	0.8941	0.9116	0.9301	0.9471	0.9620
FPTA	0.7284	0.7839	0.8257	0.8515	0.8800	0.9006	0.9176	0.9355	0.9518	0.9665
FPMA	0.6970	0.7652	0.8109	0.8395	0.8692	0.8911	0.9091	0.9277	0.9453	0.9602
OP	0.6964	0.7649	0.8105	0.8393	0.8690	0.8908	0.9088	0.9274	0.9450	0.9598

Table 24: MAE of the alternative methods for k-day-ahead forecasts when $H = 0.2$.

k	1	2	3	4	5	6	7	8	9	10
IPGA	0.7415	0.8405	0.904	0.9519	0.9897	1.0227	1.0555	1.0836	1.1082	1.1282
IPRA	0.7488	0.8423	0.9042	0.9508	0.9876	1.0205	1.0531	1.0811	1.1055	1.1253
IPTA	0.7757	0.8616	0.9200	0.9642	0.9994	1.0312	1.0627	1.0905	1.1142	1.1334
IPMA	0.7238	0.8269	0.8921	0.9411	0.9799	1.0135	1.0472	1.0751	1.1000	1.1204
FPGA	0.7417	0.8406	0.9042	0.9520	0.9898	1.0229	1.0555	1.0837	1.1083	1.1283
FPRA	0.7488	0.8423	0.9042	0.9508	0.9876	1.0205	1.0530	1.0811	1.1054	1.1252
FPTA	0.7757	0.8616	0.9200	0.9643	0.9995	1.0312	1.0627	1.0905	1.1142	1.1334
FPMA	0.7238	0.8269	0.8921	0.9411	0.9799	1.0135	1.0471	1.075	1.0999	1.1203
OP	0.7220	0.8251	0.8903	0.9392	0.9782	1.0118	1.0454	1.0733	1.0980	1.1184

Table 25: MAE of the alternative methods for k-day-ahead forecasts when $H = 0.25$.

k	1	2	3	4	5	6	7	8	9	10
IPGA	0.7861	0.9084	0.9933	1.0633	1.1228	1.1686	1.2085	1.2499	1.2898	1.3247
IPRA	0.7959	0.9107	0.9920	1.0601	1.1191	1.1640	1.2032	1.2446	1.2849	1.3191
IPTA	0.8325	0.9375	1.0142	1.0794	1.1371	1.1805	1.2182	1.2588	1.2986	1.3319
IPMA	0.7538	0.8840	0.9723	1.0438	1.1039	1.1506	1.1917	1.2338	1.2740	1.3094
FPGA	0.7861	0.9084	0.9933	1.0633	1.1228	1.1685	1.2085	1.2498	1.2898	1.3247
FPRA	0.7959	0.9106	0.9919	1.0601	1.1191	1.1638	1.2031	1.2444	1.2847	1.3190
FPTA	0.8324	0.9375	1.0142	1.0794	1.1370	1.1804	1.2181	1.2587	1.2985	1.3318
FPMA	0.7538	0.8840	0.9723	1.0437	1.1039	1.1505	1.1917	1.2337	1.2739	1.3093
OP	0.7471	0.8779	0.9669	1.0377	1.0975	1.1442	1.1859	1.2278	1.2674	1.3031

Table 26: MAE of the alternative methods for k-day-ahead forecasts when $H = 0.4$.

k	1	2	3	4	5	6	7	8	9	10
IPGA	0.9149	1.1588	1.3398	1.4880	1.6124	1.7226	1.8204	1.9147	1.9954	2.0781
IPRA	0.9349	1.1621	1.3352	1.4786	1.5993	1.7068	1.8028	1.8957	1.9755	2.0572
IPTA	1.0026	1.2181	1.3849	1.5247	1.6426	1.7482	1.8426	1.9338	2.0126	2.0931
IPMA	0.8300	1.0853	1.2713	1.4218	1.5478	1.6596	1.7585	1.8541	1.9355	2.0194
FPGA	0.9142	1.1580	1.3390	1.4870	1.6114	1.7215	1.8193	1.9135	1.9942	2.0768
FPRA	0.9345	1.1616	1.3347	1.4780	1.5986	1.7061	1.8021	1.8949	1.9746	2.0563
FPTA	1.0021	1.2175	1.3842	1.5239	1.6418	1.7473	1.8417	1.9329	2.0116	2.0921
FPMA	0.8297	1.0850	1.2709	1.4214	1.5472	1.6590	1.7579	1.8535	1.9348	2.0187
OP	0.7886	1.0405	1.2245	1.3728	1.4975	1.6096	1.7067	1.8013	1.8823	1.9663

Table 27: MAE of the alternative methods for k-day-ahead forecasts of log RV of SPY between October 1, 2017 and September 30, 2022. Boldface corresponds to the lowest MAE.

k	1	2	3	4	5	6	7	8	9	10
IPGA	0.2316	0.2716	0.2962	0.3111	0.3234	0.3343	0.3451	0.3517	0.3613	0.3700
IPRA	0.2358	0.2741	0.2964	0.3117	0.3244	0.3353	0.3459	0.3535	0.3625	0.3718
IPTA	0.2476	0.2816	0.3012	0.3159	0.3277	0.3390	0.3481	0.3562	0.3654	0.3746
IPMA	0.2211	0.2646	0.2924	0.3078	**0.3214**	**0.3325**	0.3438	0.3507	0.3599	0.3682
FPGA	0.2315	0.2715	0.2961	0.3110	0.3232	0.3342	0.3450	0.3515	0.3611	0.3698
FPRA	0.2358	0.2740	0.2964	0.3116	0.3244	0.3352	0.3458	0.3534	0.3623	0.3716
FPTA	0.2476	0.2816	0.3011	0.3158	0.3276	0.3389	0.3480	0.3561	0.3652	0.3744
FPMA	0.2211	0.2646	**0.2923**	**0.3077**	**0.3214**	**0.3325**	**0.3437**	**0.3505**	**0.3597**	**0.3680**
OP	**0.2176**	**0.2627**	0.2924	0.3089	0.3232	0.3350	0.3460	0.3537	0.3624	0.3696

Table 28: MAE of the alternative methods for k-day-ahead forecasts of XLB. Boldface corresponds to the lowest MAE.

k	1	2	3	4	5	6	7	8	9	10
IPGA	0.1691	0.1974	0.2135	0.2260	0.2379	0.2464	0.2535	0.2578	0.2634	0.2690
IPRA	0.1726	0.1985	0.2140	0.2272	0.2395	0.2480	0.2547	0.2596	0.2648	0.2709
IPTA	0.1809	0.2032	0.2176	0.2311	0.2417	0.2496	0.2558	0.2609	0.2663	0.2725
IPMA	0.1615	0.1933	0.2109	**0.2240**	**0.2368**	**0.2462**	0.2538	0.2585	0.2638	0.2693
FPGA	0.1690	0.1973	0.2134	0.2259	0.2378	0.2464	**0.2534**	**0.2577**	**0.2633**	**0.2689**
FPRA	0.1725	0.1985	0.2139	0.2271	0.2395	0.2479	0.2547	0.2595	0.2648	0.2708
FPTA	0.1809	0.2032	0.2176	0.2311	0.2417	0.2496	0.2557	0.2608	0.2662	0.2724
FPMA	0.1614	0.1932	**0.2108**	**0.2240**	**0.2368**	**0.2462**	0.2537	0.2584	0.2637	0.2692
OP	**0.1600**	**0.1921**	0.2115	0.2250	0.2384	0.2487	0.2573	0.2621	0.2679	0.2730

Table 29: MAE of the alternative methods for k-day-ahead forecasts of XLE. Boldface corresponds to the lowest MAE.

k	1	2	3	4	5	6	7	8	9	10
IPGA	0.1383	0.1632	0.1785	0.1893	**0.1988**	**0.2042**	0.2103	**0.2151**	**0.2207**	0.2256
IPRA	0.1432	0.1662	0.1803	0.1912	0.2000	0.2054	0.2117	0.2171	0.2225	0.2272
IPTA	0.1502	0.1704	0.1831	0.1939	0.2011	0.2069	0.2130	0.2183	0.2236	0.2279
IPMA	0.1324	0.1614	**0.1778**	**0.1888**	0.1992	0.2050	**0.2101**	0.2155	0.2214	0.2264
FPGA	0.1383	0.1632	0.1785	0.1893	**0.1988**	**0.2042**	0.2103	**0.2151**	**0.2207**	**0.2255**
FPRA	0.1432	0.1662	0.1803	0.1912	0.2000	0.2054	0.2117	0.2171	0.2224	0.2271
FPTA	0.1502	0.1704	0.1831	0.1939	0.2011	0.2069	0.2130	0.2183	0.2235	0.2278
FPMA	0.1324	0.1614	0.1779	**0.1888**	0.1992	0.2050	**0.2101**	0.2155	0.2214	0.2263
OP	**0.1320**	**0.1619**	0.1813	0.1914	0.2009	0.2089	0.2125	0.2176	0.2246	0.2303

Table 30: MAE of the alternative methods for k-day-ahead forecasts of XLF. Boldface corresponds to the lowest MAE.

k	1	2	3	4	5	6	7	8	9	10
IPGA	0.1639	0.1934	0.2120	0.2246	0.2359	0.2451	0.2521	0.2582	0.2629	0.2695
IPRA	0.1689	0.1956	0.2124	0.226	0.2379	0.2463	0.2536	0.2601	0.2648	0.2716
IPTA	0.1770	0.2008	0.2163	0.2296	0.2405	0.2483	0.2552	0.2612	0.2664	0.2733
IPMA	0.1565	**0.1904**	**0.2095**	**0.2221**	**0.2346**	**0.2448**	0.2523	0.2592	0.2634	0.2695
FPGA	0.1639	0.1934	0.2120	0.2246	0.2358	0.2450	**0.2520**	**0.2581**	**0.2628**	**0.2694**
FPRA	0.1688	0.1956	0.2124	0.2259	0.2378	0.2463	0.2535	0.2600	0.2647	0.2716
FPTA	0.1770	0.2008	0.2163	0.2296	0.2405	0.2482	0.2551	0.2611	0.2663	0.2733
FPMA	0.1565	**0.1904**	**0.2095**	**0.2221**	**0.2346**	**0.2448**	0.2522	0.2591	0.2633	**0.2694**
OP	**0.1551**	**0.1904**	0.2103	0.2228	0.2364	0.2475	0.2554	0.2624	0.2670	0.2730

Table 31: MAE of the alternative methods for k-day-ahead forecasts of XLI. Boldface corresponds to the lowest MAE.

k	1	2	3	4	5	6	7	8	9	10
IPGA	0.1741	0.2058	0.2256	0.2408	0.2527	0.2619	0.2702	0.2752	0.2805	0.2876
IPRA	0.1780	0.2074	0.2266	0.2422	0.2545	0.2635	0.2715	0.2772	0.2825	0.2890
IPTA	0.1874	0.2136	0.2314	0.2457	0.2572	0.2655	0.2728	0.2784	0.2841	0.2910
IPMA	0.1650	0.1999	0.2221	**0.2380**	**0.2512**	0.2618	0.2703	0.2759	0.2809	0.2871
FPGA	0.1741	0.2057	0.2256	0.2407	0.2527	0.2619	**0.2701**	**0.2751**	**0.2804**	0.2875
FPRA	0.1780	0.2074	0.2266	0.2422	0.2545	0.2635	0.2714	0.2772	0.2824	0.2889
FPTA	0.1873	0.2136	0.2314	0.2457	0.2572	0.2655	0.2728	0.2783	0.2840	0.2909
FPMA	0.1650	0.1999	0.2221	**0.2380**	**0.2512**	**0.2617**	0.2703	0.2759	0.2808	**0.2870**
OP	**0.1627**	**0.1984**	**0.2220**	0.2382	0.2527	0.2651	0.2740	0.2796	0.2849	0.2901

Table 32: MAE of the alternative methods for k-day-ahead forecasts of XLK. Boldface corresponds to the lowest MAE.

k	1	2	3	4	5	6	7	8	9	10
IPGA	0.2043	0.2361	0.2571	0.2688	0.2764	0.2837	0.2921	0.2985	0.3048	0.3112
IPRA	0.2084	0.2387	0.2579	0.2693	0.2773	0.2848	0.2926	0.2999	0.3060	0.3126
IPTA	0.2180	0.2448	0.2618	0.2715	0.2792	0.2872	0.2945	0.3019	0.3082	0.3141
IPMA	0.1967	0.2323	**0.2553**	**0.2679**	**0.2761**	**0.2834**	**0.2912**	0.2974	**0.3043**	**0.3109**
FPGA	0.2043	0.2361	0.2571	0.2688	0.2764	0.2837	0.2920	0.2985	0.3048	0.3112
FPRA	0.2084	0.2387	0.2579	0.2693	0.2772	0.2848	0.2925	0.2999	0.3060	0.3126
FPTA	0.2180	0.2448	0.2618	0.2714	0.2792	0.2871	0.2945	0.3019	0.3082	0.3141
FPMA	0.1967	0.2323	**0.2553**	**0.2679**	**0.2761**	**0.2834**	**0.2912**	**0.2973**	**0.3043**	**0.3109**
OP	**0.1955**	**0.232**	0.2566	0.2696	0.2779	0.2863	0.2933	0.2994	0.3058	0.3120

Table 33: MAE of the alternative methods for k-day-ahead forecasts of XLP. Boldface corresponds to the lowest MAE.

k	1	2	3	4	5	6	7	8	9	10
IPGA	0.1594	0.1905	0.2091	0.2237	0.2346	0.2449	0.2541	0.2612	0.2679	0.2747
IPRA	0.1638	0.1923	0.2105	0.2246	0.2361	0.2464	0.2557	0.2628	0.2698	0.2768
IPTA	0.1725	0.1977	0.2151	0.228	0.2391	0.2492	0.2577	0.2644	0.2713	0.2789
IPMA	0.1512	0.1857	**0.2053**	**0.2213**	**0.2327**	**0.2440**	**0.2538**	0.2613	0.2679	**0.2745**
FPGA	0.1594	0.1904	0.2090	0.2236	0.2346	0.2448	0.2541	**0.2611**	0.2678	0.2746
FPRA	0.1638	0.1922	0.2104	0.2246	0.2360	0.2464	0.2556	0.2627	0.2697	0.2768
FPTA	0.1725	0.1977	0.2151	0.2279	0.2391	0.2491	0.2577	0.2643	0.2713	0.2789
FPMA	0.1512	0.1856	**0.2053**	**0.2213**	**0.2327**	**0.2440**	**0.2538**	0.2612	**0.2678**	**0.2745**
OP	**0.1505**	**0.1846**	0.2055	0.2219	0.2346	0.2469	0.2569	0.2646	0.2707	0.2766

Table 34: MAE of the alternative methods for k-day-ahead forecasts of XLU. Boldface corresponds to the lowest MAE.

k	1	2	3	4	5	6	7	8	9	10
IPGA	0.1373	0.1639	0.1821	0.1938	0.2037	0.2125	0.2200	**0.2271**	**0.2334**	0.2387
IPRA	0.1403	0.1653	0.1828	0.1951	0.2049	0.2140	0.2220	0.2293	0.2353	0.2408
IPTA	0.1482	0.1709	0.1867	0.1982	0.2074	0.2160	0.2239	0.2305	0.2364	0.2420
IPMA	0.1295	0.1586	0.1778	**0.1911**	**0.2026**	**0.2116**	**0.2199**	0.2283	0.2343	0.2393
FPGA	0.1373	0.1639	0.1820	0.1938	0.2037	0.2125	0.2200	**0.2271**	**0.2334**	**0.2386**
FPRA	0.1403	0.1652	0.1828	0.1952	0.2049	0.2140	0.2220	0.2293	0.2353	0.2408
FPTA	0.1481	0.1709	0.1867	0.1982	0.2075	0.2160	0.2239	0.2305	0.2363	0.2420
FPMA	0.1295	0.1586	0.1778	**0.1911**	**0.2026**	**0.2116**	**0.2199**	0.2283	0.2343	0.2393
OP	**0.1277**	**0.1559**	**0.1763**	0.1914	0.2042	0.2131	0.2236	0.2327	0.2387	0.2438

Table 35: MAE of the alternative methods for k-day-ahead forecasts of XLV. Boldface corresponds to the lowest MAE.

k	1	2	3	4	5	6	7	8	9	10
IPGA	0.1659	0.1931	0.2102	0.2228	0.2325	0.2428	0.2500	0.2548	0.2604	0.2665
IPRA	0.1698	0.1943	0.2113	0.2240	0.2342	0.2443	0.2509	0.2565	0.2618	0.2686
IPTA	0.1778	0.1996	0.2153	0.2270	0.2374	0.2462	0.2523	0.2578	0.2632	0.2707
IPMA	0.1578	0.1892	**0.2078**	**0.2212**	**0.2313**	0.2424	0.2498	0.2553	0.2606	0.2661
FPGA	0.1659	0.1931	0.2101	0.2227	0.2324	0.2428	0.2499	**0.2547**	**0.2603**	0.2664
FPRA	0.1697	0.1943	0.2113	0.2240	0.2342	0.2442	0.2508	0.2564	0.2617	0.2686
FPTA	0.1778	0.1996	0.2153	0.2270	0.2373	0.2462	0.2523	0.2577	0.2631	0.2706
FPMA	0.1578	0.1892	**0.2078**	**0.2212**	**0.2313**	**0.2423**	**0.2497**	0.2552	0.2606	**0.2660**
OP	**0.1554**	**0.1884**	0.2087	0.2225	0.2331	0.2448	0.2521	0.2583	0.2640	0.2685

Table 36: MAE of the alternative methods for k-day-ahead forecasts of XLY. Boldface corresponds to the lowest MAE.

k	1	2	3	4	5	6	7	8	9	10
IPGA	0.2030	0.2355	0.2553	0.2673	0.2780	0.2860	0.2934	0.2975	**0.3035**	0.3079
IPRA	0.2070	0.2377	0.2556	0.2687	0.2794	0.2875	0.2939	0.2985	0.3042	0.3095
IPTA	0.2164	0.2431	0.2595	0.2721	0.2812	0.2895	0.2948	0.3005	0.3054	0.3115
IPMA	0.1946	0.2307	**0.2527**	**0.2651**	**0.2777**	0.2863	0.2938	**0.2968**	**0.3035**	**0.3071**
FPGA	0.2030	0.2355	0.2553	0.2672	0.2779	**0.2859**	**0.2933**	0.2975	**0.3035**	0.3079
FPRA	0.2070	0.2377	0.2556	0.2686	0.2793	0.2874	0.2939	0.2985	0.3041	0.3095
FPTA	0.2164	0.2431	0.2594	0.2720	0.2812	0.2895	0.2948	0.3005	0.3054	0.3115
FPMA	0.1946	0.2307	**0.2527**	**0.2651**	**0.2777**	0.2862	0.2938	**0.2968**	**0.3035**	**0.3071**
OP	**0.1933**	**0.2305**	0.2535	0.2655	0.2789	0.2885	0.2959	0.2984	0.3047	0.3078

Table 37: MAE of the alternative methods for k-day-ahead forecasts of log RV of SPY between January 2, 2012 and December 31, 2019. Boldface corresponds to the lowest MAE.

k	1	2	3	4	5	6	7	8	9	10
IPGA	0.2330	0.2611	0.2816	0.2992	0.3156	0.3284	0.3422	0.3519	0.3584	0.3667
IPRA	0.2333	0.2600	0.2807	0.2980	0.3144	0.3281	0.3415	0.3512	0.3580	0.3659
IPTA	0.2419	0.2666	0.2863	0.3034	0.3187	0.3335	0.3452	0.3542	0.3613	0.3686
IPMA	0.2242	0.2553	0.2758	0.2929	0.3109	0.3230	0.3385	0.3489	0.3556	0.3639
FPGA	0.2330	0.2610	0.2815	0.2992	0.3156	0.3283	0.3421	0.3518	0.3583	0.3666
FPRA	0.2333	0.2600	0.2806	0.2979	0.3144	0.3280	0.3415	0.3511	0.3579	0.3658
FPTA	0.2418	0.2666	0.2862	0.3034	0.3187	0.3334	0.3451	0.3541	0.3612	0.3685
FPMA	0.2242	0.2552	0.2758	0.2929	0.3108	0.3229	0.3385	0.3489	**0.3555**	0.3638
OP	**0.2222**	**0.2541**	**0.2746**	**0.2910**	**0.3097**	**0.3219**	**0.3381**	**0.3483**	0.3557	**0.3637**

References

Andersen, T. G., Bollerslev, T., Diebold, F. X., Labys, P., 2003. Modeling and forecasting realized volatility. *Econometrica* 71(2), 579–625.

Barndorff-Nielsen, O. E., Corcuera, J. M., Podolskij, M., 2013. Limit theorems for functionals of higher order differences of Brownian semi-stationary processes. In *Prokhorov and Contemporary Probability Theory: In Honor of Yuri V. Prokhorov*, Volume 33, 69–96. Springer Science & Business Media.

Bayer, C., Friz, P., Gatheral, J., 2016. Pricing under rough volatility. *Quantitative Finance* 16(6), 887–904.

Bennedsen, M., Christensen, K., Christensen, P., 2022. Likelihood-Based Estimation of Rough Stochastic Volatility Models, Aarhus University, manuscript.

Bolko, A. E., Christensen, K., Pakkanen, M. S. , and Veliyev, B. (2023). A GMM approach to estimate the roughness of stochastic volatility. *Journal of Econometrics*, forthcoming.

Brouste, A., Soltane, M., Votsi, I., 2020. One-step estimation for the fractional Gaussian noise at high-frequency. *ESAIM: Probability and Statistics* 24, 827–841.

Corsi, F., 2009. A simple approximate long-memory model of realized volatility. *Journal of Financial Econometrics* 7(2), 174–196.

Diebold, F.X., R. S. Mariano 1995. Comparing Predictive Accuracy, *Journal of Business & Economic Statistics*, 13(3), 253-263

Euch, O. E., Rosenbaum, M., 2018. Perfect hedging in rough Heston models. *Annals of Probability* 28(6), 3813–3856.

Fukasawa, M., T. Takabatake, and R. Westphal, 2022. Consistent estimation for fractional stochastic volatility model under high-frequency asymptotics. *Mathematical Finance*, 32(4), 1086-1132.

Fouque, J. P., Hu, R., 2018. Optimal portfolio under fast mean–reverting fractional stochastic environment. *SIAM Journal of Financial Mathematics* 9(2), 564–601.

Garnier, J., Sølna, K., 2017. Correction to Black-Scholes formula due to fractional stochastic volatility. *SIAM Journal Financial Mathematics* 8(1), 560–588.

Gatheral, J., Jaisson, T., Rosenbaum, M., 2018. Volatility is rough. *Quantitative Finance* 18(6), 933–949.

Lang, G., Roueff, F., 2001. Semi-parametric estimation of the Hölder exponent of a stationary Gaussian process with minimax rates. *Statistical Inference for Stochastic Processes* 4(3), 283–306.

Livieri, G., Mouti, S., Pallavicini, A., Rosenbaum, M., 2018. Rough volatility: evidence from option prices. *IISE Transactions* 50(9), 767–776.

Mandelbrot, B.B., Van Ness, J.W., 1968. Fractional Brownian motions, fractional noises and applications. *SIAM Review*. 10, 422–437.

Nuzman, C. J., Poor, H. V., 2000. Linear Estimation of Self-Similar Processes via Lamperti's Transformation. *Journal of Applied Probability*, 37(2), 429-452.

Shi, S., Yu, J., Zhang, C., 2023. On the Spectral Density of Fractional Ornstein-Uhlenbeck Process: Approximation, Estimation, and Model Comparison. *SMU Economics and Statistics Working Paper Series*.

Tallarida, R. J., 2015. *Pocket Book of Integrals and Mathematical Formulas*. 5th Edition, Taylor & Francis Group.

Wang, X., Xiao, W., Yu, J., 2023. Modeling and Forecasting Realized Volatility with the Fractional Ornstein-Uhlenbeck Process. *Journal of Econometrics*, 232(2), 389-415.